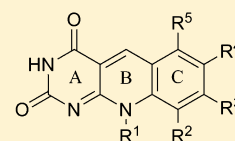
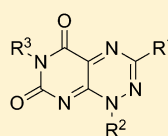


Toxoflavins and Deazaflavins as the First Reported Selective Small Molecule Inhibitors of Tyrosyl-DNA Phosphodiesterase II

Ali Raoof,^{*,†} Paul Depledge,[†] Niall M. Hamilton,[†] Nicola S. Hamilton,[†] James R. Hitchin,[†] Gemma V. Hopkins,[†] Allan M. Jordan,[†] Laura A. Maguire,[†] Alison E. McGonagle,[†] Daniel P. Mould,[†] Mathew Rushbrooke,[§] Helen F. Small,[†] Kate M. Smith,[†] Graeme J. Thomson,[†] Fabrice Turlais,[§] Ian D. Waddell,[†] Bohdan Waszkowycz,[†] Amanda J. Watson,[†] and Donald J. Ogilvie[†][†]Cancer Research UK Drug Discovery Unit, Paterson Institute for Cancer Research, University of Manchester, Wilmslow Road, Manchester M20 4BX, U.K.[§]Cancer Research Technology Ltd., Wolfson Institute for Biomedical Research, The Cruciform Building, Gower Street, London WC1E 6BT, U.K.

S Supporting Information

ABSTRACT: The recently discovered enzyme tyrosyl-DNA phosphodiesterase 2 (TDP2) has been implicated in the topoisomerase-mediated repair of DNA damage. In the clinical setting, it has been hypothesized that TDP2 may mediate drug resistance to topoisomerase II (topo II) inhibition by etoposide. Therefore, selective pharmacological inhibition of TDP2 is proposed as a novel approach to overcome intrinsic or acquired resistance to topo II-targeted drug therapy. Following a high-throughput screening (HTS) campaign, toxoflavins and deazaflavins were identified as the first reported sub-micromolar and selective inhibitors of this enzyme. Toxoflavin derivatives appeared to exhibit a clear structure–activity relationship (SAR) for TDP2 enzymatic inhibition. However, we observed a key redox liability of this series, and this, alongside early *in vitro* drug metabolism and pharmacokinetics (DMPK) issues, precluded further exploration. The deazaflavins were developed from a singleton HTS hit. This series showed distinct SAR and did not display redox activity; however low cell permeability proved to be a challenge.



INTRODUCTION

Topoisomerases are nuclear enzymes involved in the movement of DNA within the nucleus or in the opening of the double helix. These enzymes generate reversible breaks in DNA thereby allowing DNA decatenation. In order to carry out its critical physiological functions, topoisomerase generates transient topoisomerase–DNA cleavage complexes, so-called cleavable complexes, in DNA. Oxidation, ionizing radiation, or chemotherapeutic agents can stabilize this complex and prevent the enzyme from resealing the DNA break it creates, resulting in topoisomerase enzyme-mediated DNA damage.¹ Topo II poisons such as etoposide can induce abortive DNA strand breaks in which topo II remains covalently bound to a 5' DNA strand terminus via a phosphotyrosyl linker (Figure 1).^{3–8} TDP2 (EC 3.1.4., aka TTRAP, EAPII)² is a recently discovered human 5'-tyrosyl-DNA phosphodiesterase, and it has been proposed that TDP2 may remove degraded topo II peptides covalently linked to the 5' terminus, thus playing a central role in maintaining normal DNA topology in cells (Figure 1).^{6–9} Cellular depletion of TDP2 has been shown to result in an increased susceptibility and sensitivity of cells to topo II-induced DNA double-strand breaks, thereby suggesting TDP2 as a potentially attractive anticancer target.¹

A chromogenic enzymatic assay for TDP2, using 4-nitrophenyl phenylphosphonate (NPPP) as the substrate,¹ was developed for a high-throughput screen comprising

approximately 100 000 compounds assembled from a variety of commercial compound suppliers, where 85% of the compounds were chemically diverse and the remaining 15% screened were from a commercial kinase inhibitor collection. The commercially available β -lapachone, RO 08-2750, and NSC95397 were employed as the positive controls (with IC₅₀'s of 0.97, 3.5, and 71 μ M, respectively). Subsequent in-house resynthesis and reconfirmation of hits resulted in toxoflavins and a singleton deazaflavin emerging as confirmed hits. Selectivity screening against the related phosphodiesterases tyrosyl-DNA phosphodiesterase 1 (TDP1) and apurinic/apyrimidinic endonuclease (APE-1) was carried out to facilitate an initial assessment of selective pharmacological inhibition by the two chemical series. While TDP1 is mechanistically and structurally different from TDP2, it catalyzes a similar phosphodiester bond cleavage and is the closest equivalent enzyme in terms of function and homology.¹⁰ However, despite this perceived similarity, TDP2 and TDP1 actually perform very different cellular roles and as such should be considered as separate target family classes.² APE-1, like TDP1, is a DNA repair enzyme and shares the closest known three-dimensional shape and folding pattern compared with TDP2.¹¹

Received: January 29, 2013

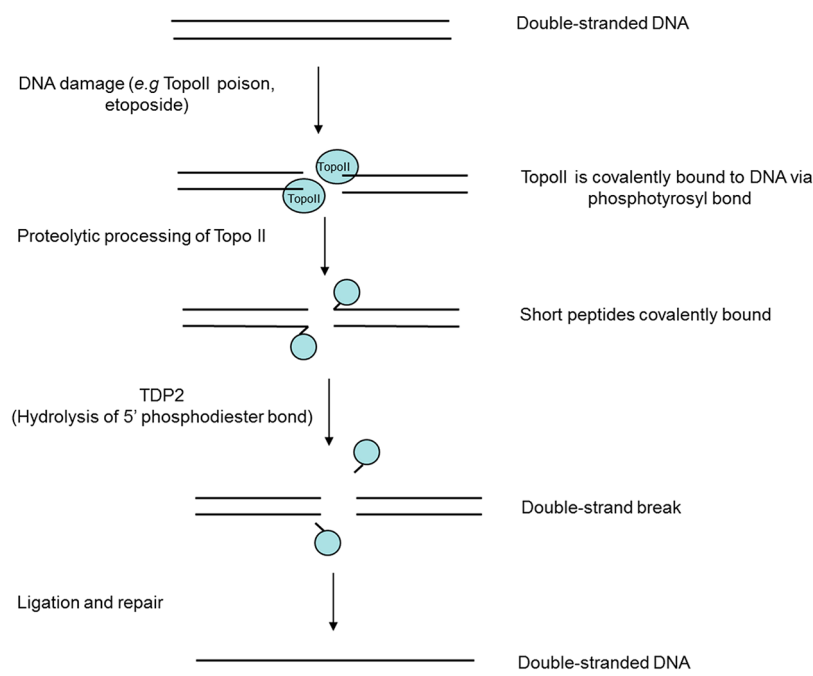


Figure 1. The roles of Topo II and TDP2.

Previous to our work, the less potent 5-arylideneethiothiazolidinones were reported as TDP1 inhibitors.¹² Although submicromolar activities for TDP1 inhibition have been reported, the selectivity and hence potency against TDP2 for the reported chemical series may require further optimization in order to establish clear pharmacological inhibition.

Toxoflavins were first isolated as toxins produced by bacteria including *Burkholderia gladioli*¹³ and are precedented in the literature as potential antibiotics¹⁴ and chemotherapeutic agents.^{15,16} The use of these compounds in the treatment of other diseases such as asthma and diabetes has also been reported in the patent literature.^{17,18} The toxoflavins exhibit structural features reminiscent of xanthines such as theophylline, a competitive nonselective phosphodiesterase inhibitor,¹⁹ suggesting that toxoflavins could inhibit TDP2 activity. Further, the pyrimidodione moiety of toxoflavins may act as a phosphate mimetic,²⁰ hence providing an avenue for scaffold hopping.

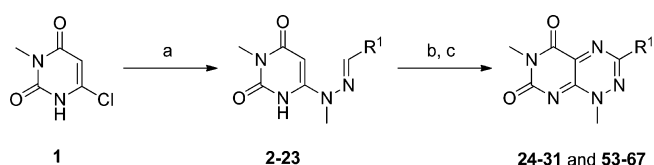
Deazaflavins were first discovered as derivatives of the biochemically significant flavins²¹ and have recently been shown to exhibit antitumor and antiproliferative activity.^{22,23}

In this study, we explore the drug-like nature of both the toxoflavins and deazaflavins as the first potent and selective small molecule inhibitors of the TDP2 enzyme.

CHEMISTRY

The synthesis of key SAR compounds is summarized in Schemes 1–12. The toxoflavins were prepared following adaptations of literature protocols.²⁴ R¹ variations were introduced by reaction of methyl hydrazine with the commercially available 6-chloro-3-methyluracil **1**, followed by condensation with a range of aldehydes to furnish the intermediate hydrazones **2–23** in respectable yields. Triazine formation was achieved by treatment of the hydrazones **2–23** with sodium nitrite under acidic conditions, followed by DTT reduction of the N-oxide to give the toxoflavins **24–31** and **53–67** (Scheme 1).

Scheme 1^a



^aReagents: (a) (i) MeNHNH₂, EtOH, μ W, 100 °C, 10 min; (ii) RCHO, 50 °C, 10 min (32–100%); (b) NaNO₂, AcOH, H₂O, ambient temperature, 16 h; (c) 1,4-bis(sulfanyl)butane-2,3-diol, EtOH, reflux, 1 h (1–82%).

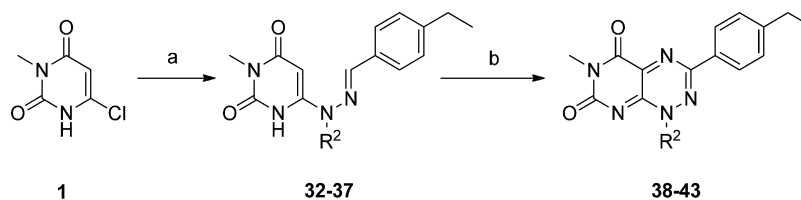
Toxoflavin R² modifications for compounds **38–43** were prepared utilizing a similar procedure as that illustrated in Scheme 1 where the R² diversity was introduced by varying the hydrazine building blocks while maintaining the R¹ functionality as the 4-ethylphenyl (Scheme 2).²⁴

Appropriately substituted ureas were the source of toxoflavin R³ variations for compounds **50–52**. R³ substituted chlorouracils **44–46** were reacted in similar manner to 6-chloro-3-methyluracil **1** to furnish the desired products in respectable yields (Scheme 3).

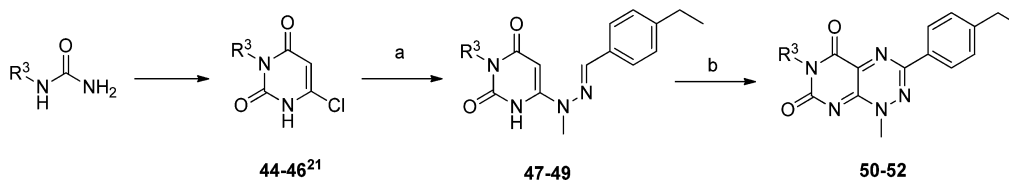
Toxoflavin heteroatom deletion compounds were prepared according to the literature (see Figure 4 for structural formulas). The commercially available R² deletion compound **69** was isolated as a byproduct from the DTT reduction of the N-oxide **68**. Deazatoxoflavin **70** was synthesized by reaction of the hydrazone intermediate **32** with the commercially available 2-bromo-1-(4-ethylphenyl)ethanone (Scheme 4).²⁵

Commercially available 6-amino-1,3-dimethyl-2,4(1H,3H)-pyrimidinedione **71** was condensed with 4-ethylbenzaldehyde to furnish the intermediate hydrazone **72**, which was treated with an ethyl formate equivalent to give the pteridine **73** (Scheme 5).²⁶

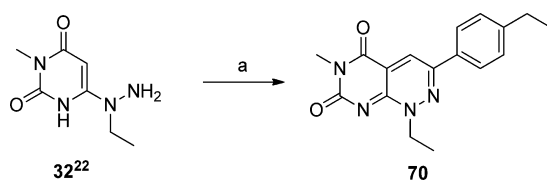
Core variation **77** was prepared from the commercially available 2-amino-6-chloro-1H-pyrimidin-4-one **74** in manner analogous to the toxoflavins (Scheme 6).²⁴

Scheme 2^a

^aReagents: (a) (i) RNHNH₂ salt, Et₃N, EtOH, reflux, 16 h; (ii) *p*-ethylbenzaldehyde 27–100%; (b) (i) NaNO₂, AcOH, water, ambient temperature, 4 h; (ii) 1,4-bis(sulfanyl)butane-2,3-diol, ambient temperature, 1 h, 27–58%.

Scheme 3^a

^aReagents: (a) (i) MeNHNH₂, EtOH, μ W, 100 °C, 10 min; (ii) 4-ethylbenzaldehyde, μ W, 50 °C, 10 min, 69–86%; (b) (i) NaNO₂, AcOH, water, ambient temperature 16 h; (ii) 1,4-bis(sulfanyl)butane-2,3-diol, ambient temperature, 10 min, 39–67%.

Scheme 4^a

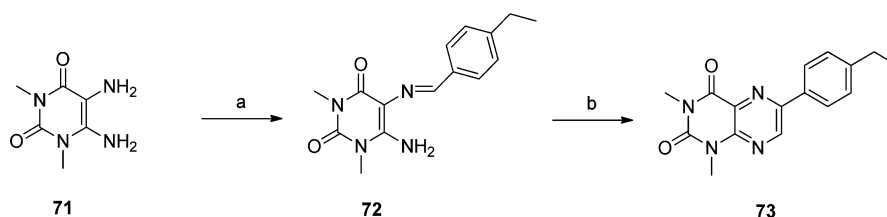
^aReagents: (a) 2-bromo-1-(4-ethylphenyl)ethanone, 2-methoxyethanol, pressure tube, 120 °C, 16 h, 0.6%.

The intermediate hydrazone **75** was also heated with ethyl phenylglyoxylate in ethanol to furnish the amino pyrimido pyridazine dione **78** (Scheme 7).²⁷

Although the hydroxy pyrimidone **82** could be prepared from the benzyl ether precursor **81** (Scheme 8) via TFA cleavage of the benzyl protecting group, chemical instability prevented isolation of the clean authentic product.²⁸

The commercially available thiophene carboxylic acid **83** was coupled to ethyl piperidine-3-carboxylate followed by ester saponification in quantitative yields (Scheme 9). Acid chloride activation and reaction with trimethyl phosphite furnished the keto phosphate **86**.²⁹

The bis arylated thiophene methyl esters **89** and **90** were prepared from 2,4-dibromothiophene **88**. Saponification to the corresponding carboxylic acids **91** and **92** and reaction with methanesulfonamide furnished the desired sulfonamide amides **93** and **94**, respectively (Scheme 10).^{30,31}

Scheme 5^a

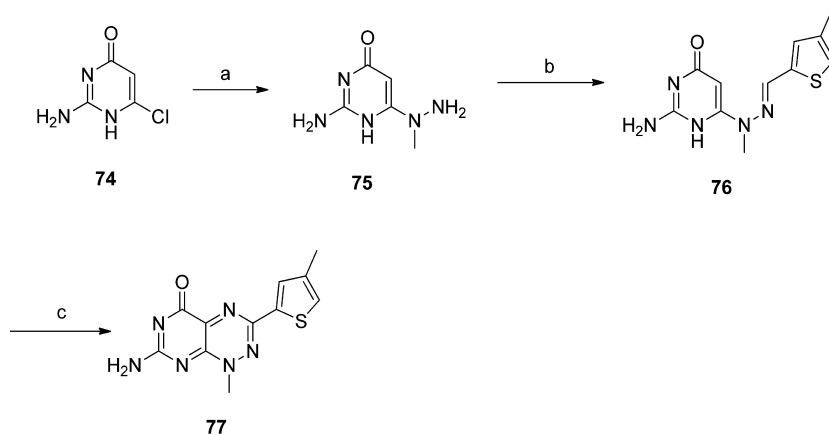
^aReagents: (a) 4-ethylbenzaldehyde, EtOH, reflux, 3 h, 63%; (b) triethoxyethane, TsOH (cat.), DMA, 120 °C, 16 h, 2%.

4-(3,4-Dimethoxyphenyl)thiophen-2-amine hydrochloride **95** was derivatized to yield aromatic amides **96–103** via acid chloride formation or EDCI activation and as a phenyl urea **104** (Scheme 11).³²

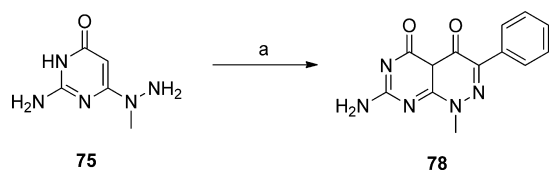
The deazaflavins **128–163** were prepared following literature precedent.^{33–43} The general procedure involved the reactions of appropriate amines with 6-chlorouracil **47** to afford the amino uracils **106–127**, which were used crude in the subsequent S_NAr and aldehyde condensation steps to furnish the desired deazaflavins (Scheme 12).

RESULTS AND DISCUSSION

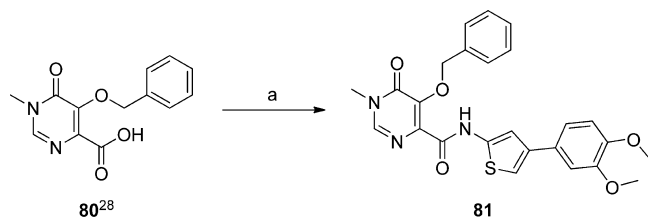
Having identified preliminary inhibitors of the TDP2 enzyme from the HTS, the synthesis of further analogues of toxoflavins was initiated. The most potent hit from the screen, the 4-chlorophenyl derivative **24**, was initially investigated. The importance of the 4-chloro substituent was evident from the des-chloro compound **25** and the 4-ethylphenyl derivative **26**. The electronics of the 4-chloro substituent had less of an impact on potency compared with the 4-trifluoromethyl analogue **27**. The three points of diversity (R¹, R², and R³) were subsequently explored (see Table 1). Early SAR for the R¹ position indicated that 4- and 3-substituted phenyls, for example, **29** and **30**, respectively, were superior to the 2-substituted analogues such as **31**. Substituents around the R² and R³ positions were less tolerated compared with those at R¹. Small alkyl variations such as ethyl and ⁿpropyl, **38** and **40**, respectively, were best tolerated at R². Surprisingly, substitution

Scheme 6^a

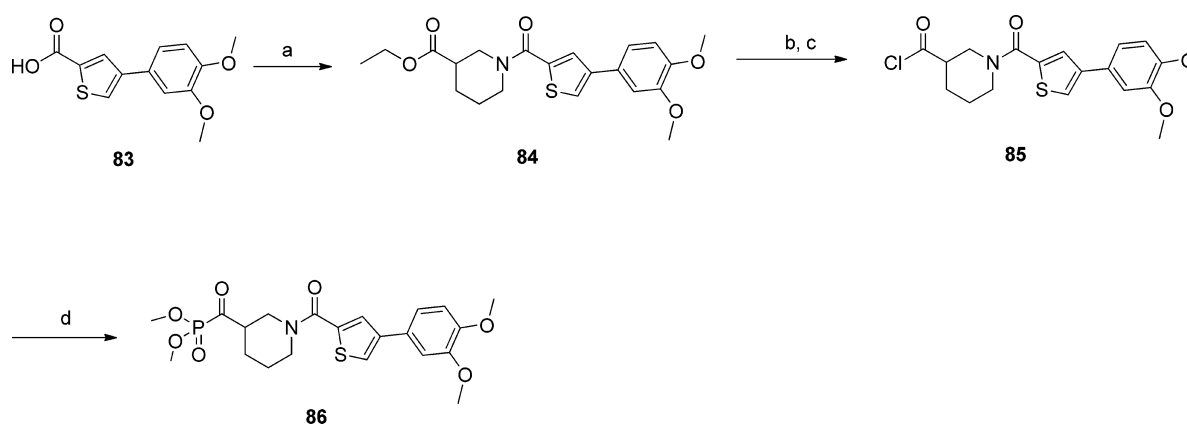
^aReagents: (a) MeNHNH₂, EtOH, reflux, 4 h, 80%; (b) 4-methylthiophene-2-carbaldehyde, EtOH, μ W, 50 °C, 10 min, 75%; (c) (i) NaNO₂, AcOH, water, ambient temperature, 4 h; (ii) 1,4-bis(sulfanyl)butane-2,3-diol, water, 50 °C, 2 h, 3%.

Scheme 7^a

^aReagents: (a) ethyl phenylglyoxylate, EtOH, reflux, 22 h, 32%.

Scheme 8^a

^aReagents: (a) EDCI, HOBT, DIPEA, 4-(3,4-dimethoxyphenyl)thiophen-2-amine hydrochloride, DMF, 0 °C to ambient temperature, 72 h, 91%.

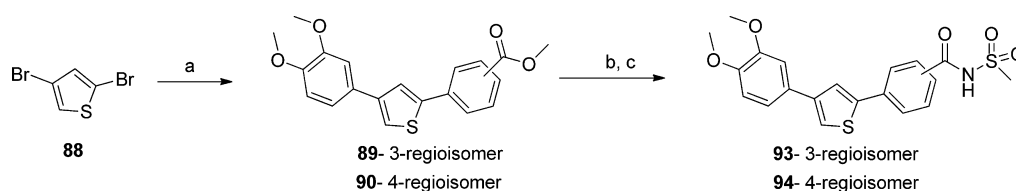
Scheme 9^a

^aReagents: (a) (i) CDI, DMF, ambient temperature, 2 h; (ii) ethyl piperidine-3-carboxylate, 100 °C, 16 h, 100%; (b) LiOH, THF, water, ambient temperature, 2 h, 100%; (c) (COCl)₂, DMF, DCM, ambient temperature, 16 h, 96%; (d) P(OMe)₃, toluene, 0 °C to ambient temperature, 72 h, 16%.

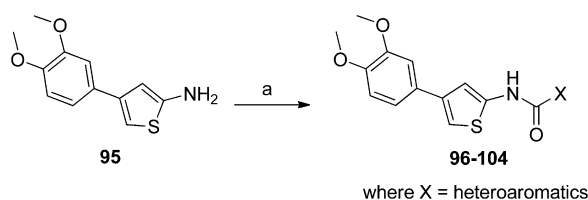
with the cyclopropyl **39** at the R² position proved detrimental compared with the methylene cyclopropyl **41**, and this might be attributed to the more sp²-like character of the directly linked cyclopropyl group. This was further supported by the inactive phenyl derivative **42**. Exemplification at the R³ position proved synthetically challenging. Limited SAR in this area indicated that the original methyl substituted compounds were clearly preferable.

Of note, all the toxoflavins prepared showed excellent selectivity against the closely related TDP1 and APE-1 enzymes (IC₅₀ > 200 μ M for APE-1 inhibition and <30% inhibition at 100 μ M for TDP1).⁴⁴

Synthetic tractability and the resultant incorporation of substructure diversity at the R¹ position was much more facile and allowed for further elaboration of the toxoflavins (Table 2), with the aim to improve potency, maintain selectivity, and initiate drug metabolism and pharmacokinetics (DMPK) investigations. In order to reduce the aromatic ring count, alkyl and cycloalkyl compounds **53–58** were synthesized. There was no significant improvement in the potencies of these compounds compared with **26**. The subsequent strategy involved further extending the R¹ position, first by introducing

Scheme 10^a

^aReagents: (a) (i) Pd(PPh₃)₄, Na₂CO₃ (aq), methoxycarbonylphenyl boronic acid, DMF, 80–90 °C, 3 h; (ii) 3,4-dimethoxybenzeneboronic acid, 80–90 °C, 16 h, 20–22%; (b) carboxylic acids **91** or **92**, LiOH, MeOH (aq), reflux, 5 h, 69–77%; (c) methanesulfonamide, EDCI, DMAP, THF, ambient temperature, 16 h, 2%.

Scheme 11^a

^aReagents: (a) for **96–102**, (i) carboxylic acid, SOCl₂, reflux, 5 h, (ii) 4-(3,4-dimethoxyphenyl)thiophen-2-amine hydrochloride **95**, DIPEA, DMAP, THF, ambient temperature, 1 h, 4–47%; For **103**, (i) 4-(3,4-dimethoxyphenyl)thiophen-2-amine hydrochloride **95**, DIPEA, DMF, 0 °C, 15 min, (ii) 4,6-dimethyl-2-oxo-2H-pyran-5-carboxylic acid, EDCI, ambient temperature, 16 h, 16%; for **104**, phenyl isocyanate, 4-(3,4-dimethoxyphenyl)thiophen-2-amine hydrochloride **95**, DIPEA, DCM, ambient temperature, 10 min, 17%.

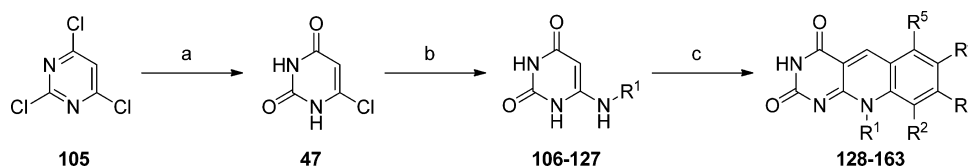
aliphatic linkers to the phenyl ring, for example, compounds **56** and **57**. This disruption of planarity and aromaticity had little impact on potency compared with the directly linked phenyl **25**. Although the heteroaromatic replacement of the phenyl ring **25** with the 3-thiazole functionality **63** was also detrimental in terms of potency, improvements were made by further substitution on the heteroaromatic ring. Optimized potency, while retaining TDP1 and APE-1 selectivity,⁴⁴ was delivered by increasing the substituent size on the thiophene R¹ group from methyl **64** to phenyl **66** or 3,4-dimethoxyphenyl **67**.

At this stage, early *in vitro* DMPK of the toxoflavins was assessed. Increasing the lipophilicity and hence calculated log *P*⁴⁵ of the toxoflavins core resulted in a decrease in both solubility and permeability (Table 3). The initial key compound, **26**, exhibited good aqueous solubility and Caco-2 permeability⁴⁶ and at first glance appeared to demonstrate good stability in human liver microsomes. However <1 μM inhibition of the standard cytochrome P450 isoforms (CYPs) inferred that this high stability was possibly a consequence of the saturation of the CYP enzymes, preventing metabolic degradation.

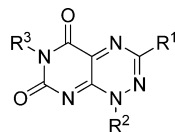
Toxoflavins heteroatom deletion compounds **69**, **70**, and **73** were prepared in an attempt to retain potency and design out

cytochrome P450 liabilities of the toxoflavins core. These compounds failed to retain activity compared with the toxoflavins series (Figure 2). More elaborate changes to the toxoflavins core were subsequently investigated. While the aminopyrimidone replacement **77** exhibited micromolar activity and low permeability, an efflux liability became apparent compared with the parent toxoflavins (Figure 2). The aminopyrimidone series was further modified to replace a triazine nitrogen with a carbonyl functionality (**78**). Single point enzyme inhibition data indicated substantial loss of activity compared with **77** (Figure 2). Additionally, the commercially available tetrahydrofolate **79**, which was reminiscent of the amino pyrimidone **77**, was also relatively inactive (Figure 2).

In the absence of a crystal structure for TDP2, it was postulated that the toxoflavins core may be acting as a nucleotide mimetic stacking against the substrate DNA bases, or possibly as a phosphate mimetic, with the pyrimidodione lone pair electrons involved in binding to Mg/Mn metal ions in the enzyme active site. With this in mind, the thiophene dimethoxy phenyl fragment of the most potent toxoflavins **67** was coupled to a small selection of phosphates and phosphate mimetics²⁰ in an attempt to eliminate the cytochrome P450 liabilities. A small library of replacements for the pyrimidodione core were modeled using the Maestro software package from Schrodinger.⁴⁷ The overall three-dimensional similarity was evident by aligning to the parent compound **67** using the Torch software from Cresset,⁴⁸ which assesses similarity in terms of shape and properties, where a score of 0.7 or greater was considered a “good” score (Figure 3). Disappointingly, the hydroxy pyrimidone **82** proved to be chemically unstable, and the benzyl ether precursor **81** was inactive compared with the toxoflavins **67**. Attempts to prepare a phosphate with an adjacent gem-difluoro functionality, **87**, in order to modify the p*K*_a of the molecule proved difficult. However, a keto-phosphate analogue **86** was synthesized, but again also lacked activity. The 3- and 4-phenyl sulfonamide amides, **93** and **94**, respectively, also resulted in the complete loss of activity (Figure 3).

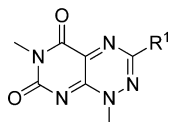
Scheme 12^a

^aReagents: (a) NaOH (aq), reflux, 2 h, 98%; (b) R¹NH₂, *n*-propanol, μW, 150 °C, 30 min to 10 h, 45–100%; (c) substituted 2-fluorobenzaldehyde, DMF, μW, 110 °C, 10 min to 1 h, 2–86%.

Table 1. Initial Toxoflavins SAR: R¹, R², and R³ Modifications

compound	R ¹	R ²	R ³	EC ₅₀ (μM) ^a
24	4-chlorophenyl	methyl	methyl	0.43(0.15)
25	phenyl	methyl	methyl	0.78(0.20)
26	4-ethylphenyl	methyl	methyl	0.28(0.25)
27	4-(trifluoromethyl)phenyl	methyl	methyl	0.33(0.13)
28	4-(trifluoromethoxy)phenyl	methyl	methyl	0.26(0.08)
29	4-tolyl	methyl	methyl	0.29(0.12)
30	3-tolyl	methyl	methyl	0.40(0.05)
31	2-tolyl	methyl	methyl	1.07(0.10)
38	4-ethylphenyl	ethyl	methyl	0.30(0.10)
39	4-ethylphenyl	cyclopropyl	methyl	4.63(0.60)
40	4-ethylphenyl	ⁿ propyl	methyl	0.28(0)
41	4-ethylphenyl	methylenecyclopropyl	methyl	0.36(0.05)
42	4-ethylphenyl	phenyl	methyl	>10(0)
43	4-ethylphenyl	benzyl	methyl	7.42(0.65)
50	4-ethylphenyl	methyl	hydrogen	0.67(0.09)
51	4-ethylphenyl	methyl	phenyl	1.02(0.28)
52	4-ethylphenyl	methyl	benzyl	0.70(0.07)

^aValues stated are a geometric mean of at least two independent determinations with standard deviations given in parentheses. The inhibition values were expressed as EC₅₀ values rather than IC₅₀ values, because all inhibitory compounds tested showed a maximum inhibition of 75%, reaching a plateau at this level. All inhibitory compounds show hill slopes approximating unity. Example dose–response curves of representative toxoflavins can be found in the Supporting Information.

Table 2. Toxoflavin R¹ SAR Expansion

compound	R ¹	EC ₅₀ (μM) ^a
53	methyl	1.16(0)
54	ⁿ propyl	0.51(0.23)
55	cyclopropyl	0.37(0.04)
56	cyclopentyl	0.64(0.08)
57	cyclohexyl	0.75(0.19)
58	4-tetrahydropyran	0.43(0)
25	phenyl	0.78(0.20)
59	benzyl	0.96(0.05)
60	phenethyl	0.68(0.08)
61	2-naphthyl	0.15(0.01)
62	3,4-dimethoxyphenyl	0.87(0.97)
63	3-thiazol	0.77(0.08)
64	4-methyl-2-thienyl	0.25(0)
65	4-bromo-2-thienyl	0.20(0.03)
66	4-phenyl-2-thienyl	0.12(0.01)
67	4-(3,4-dimethoxyphenyl)-2-thienyl	0.05(0.01)

^aValues stated are a geometric mean of at least two independent determinations with standard deviations given in parentheses. The inhibition values were expressed as EC₅₀ values rather than IC₅₀ values because all inhibitory compounds tested showed a maximum inhibition of 75%, reaching a plateau at this level. All inhibitory compounds show hill slopes approximating unity. Example dose–response curves of representative toxoflavins can be found in the Supporting Information.

Because replacing the pyrimidopyrimidinone portion of the toxoflavin core with phosphate or phosphate mimetics was

met with little success, Cresset Spark software⁴⁹ was then employed to design *de novo* toxoflavin core mimetics. The highest scoring solutions (all >0.8) were subsequently synthesized. In comparison to the toxoflavin 67, all such core hops were relatively inactive, exhibiting potencies of >30 μM in the TDP2 assay (Figure 4).

While these studies were ongoing, we became aware of a single report that toxoflavin derivatives may undertake redox cycling in the presence of DTT, which was also present in our assay to enhance TDP2 activity.⁵⁰ This report suggested that high concentrations of hydrogen peroxide could be generated *in situ* in the assay system. This may result in misleading assay interpretations, although the inclusion of DTT present in the counter screen versus TDP1 and APE-1 showed that the toxoflavins were relatively inactive against these enzymes.⁴⁴ To this end, we conducted an assessment of the redox potential of these derivatives by measuring hydrogen peroxide generation in our assay conditions (Figure 5).⁵¹ It was evident from this assessment that the toxoflavins were indeed participating in a redox cycling interaction in the TDP2 enzymatic assay. Further, the levels of generated peroxide correlated well with apparent inhibitory activities in the TDP2 assay system, because the inactive toxoflavin deletion compounds 69, 70, and 73 did not display redox activity (Figure 6). These data supported the hypothesis that it was the toxoflavin core itself exhibiting redox liabilities, strongly implying that, although the SAR observed appeared sensible and credible, these data were compromised in the context of the design of TDP2 inhibitors.

In summary for this series, the medicinal chemistry design of exemplified toxoflavins led to apparently potent and selective inhibitors with undesirable cytochrome P450 liabilities. The redox assay interference was hoped to have been alleviated by replacing the toxoflavin core. However, all synthetic variations

Table 3. Toxoflavins *in Vitro* DMPK

compound	xLogP	aqueous solubility (μM) ^a	$P_{a \rightarrow b}$ ^b (10^{-6} cm s ⁻¹)	$P_{b \rightarrow a}/P_{a \rightarrow b}$ ^b	$T_{1/2}$ ^c (min)	CYP inhibition ^d
26	1.26	100	22	0.48	455	1A2 1.5 μM ; 2C19, 2C9, 2D6, 3A4 <1 μM
28	1.93	30–100	18	0.46	325	e
52	2.99	3–10	0.7	0.23	227	e
67	2.35	3–10	0.3	0.25	e	e

^aTurbidimetric aqueous solubility: concentration of test compound that produces an increase in absorbance above 1% DMSO in buffer. ^b $P_{a \rightarrow b}$ is the permeability when applied to the apical side, while $P_{b \rightarrow a}$ is the permeability when applied to the basolateral side in a Caco-2 membrane assay. The ratio of these two values is a measure of Pgp efflux, while the $P_{a \rightarrow b}$ value is a measure of permeability. ^cMetabolic stability in human liver microsomes: half-life ($T_{1/2}$). ^dCYP (cytochrome P450) inhibition of the five standard isoforms measured as an IC_{50} . ^eNot determined.

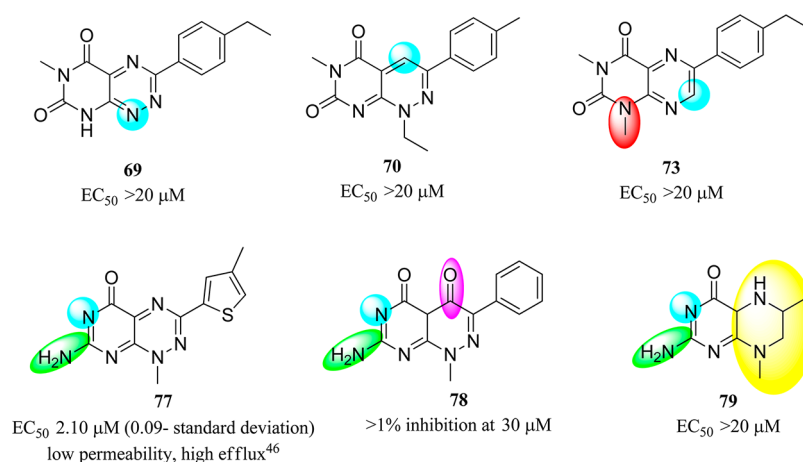


Figure 2. Toxoflavin heteroatom deletions and core variations.

resulted in the loss of activity consistent with the redox hypothesis. The subsequent focus of the study was therefore to explore additional HTS hit matter, in this instance the deazaflavins, as a potential hit series.

The deazaflavin series emerged from a singleton HTS hit, 128, exhibiting sub-10 μM potency. The unsubstituted core 129 and close analogues from the HTS (see compounds 129, 131, and 132 (Table 4)) were relatively inactive, inferring steep SAR. N-Methylation of the pyrimidodione moiety to furnish 133 also resulted in the loss of activity, in contrast to the optimized R³ methyl of the pyrimidodione of toxoflavins, implying that the SAR from the toxoflavins did not cross over to the deazaflavins.

The significance of the R³ chloro substituent required further investigation. Monochloro regioisomers around the C-ring were prepared (134–136); however these all resulted in the loss of activity, indicating the R³ chloro substituent to be important. Varying the pendant phenyl ring at R¹ with alkyl and cycloalkyl substituents (137–140) also proved detrimental to maintaining potency. Substituted phenyls were therefore synthesized in an attempt to establish further SAR. This approach was successful, because clear SAR of hydroxyphenyls 141, 143, and 144 emerged, with the 3-hydroxyphenyl 143 proving to be the most potent of the three derivatives. Biochemical assessment against TDP1 and APE-1 enzymes demonstrated complete selectivity for all derivatives exhibiting IC_{50} results less than 1 μM in the TDP2 assay (<20% inhibition at 30 μM for TDP1 and APE-1 enzymes).⁴⁴ Replacing the hydroxyl of 141 with a methoxy to give 142, and thus losing the potential for hydrogen bonding interactions, resulted in loss of activity. In order to explore electronics, substitution of the R³ chloro with the bioisosteric trifluoromethyl and nitrile moieties successfully furnished the more potent analogues 145 and 146,

respectively (Table 4). Reassuringly, after early assessment, the deazaflavins with a range of potencies did not appear to be causing redox cycling in the TDP2 enzymatic assay, giving confidence that the observed SAR was truly pharmacologically relevant (Figure 7).

Combining the optimal R¹ 3-hydroxyphenyl with the R³ nitrile proved fruitful; the SAR appeared additive and afforded compound 147 as a 0.05 μM inhibitor of the TDP2 enzyme. Further SAR was established for the deazaflavins, whereby hydrogen bonding substituents at the 3- and 4-positions of the R¹ phenyl and nitrile at the R³ position of the C ring resulted in the most potent TDP2 inhibitors (Table 4).

The pharmacological inhibition of the TDP2 enzyme by deazaflavins was further supported by an orthogonal biochemical assay using a more physiologically relevant oligonucleotide substrate.¹ In comparison to the chromogenic assay employing NPPP as the substrate, the rank order of the range of potencies for the two assays were in very good correlation. (Table 5, Figure 9).

Taken together, the use of these two new TDP2 assays has been successfully employed to identify novel small molecule inhibitors of this enzyme. Furthermore these compounds were shown to be selective over both APE-1 and TDP1. For the latter enzyme, we took advantage of a newly developed assay, which measured the AP-cleavage activity of TDP1.⁴⁴ Although not directly measuring the 3'-tyrosyl phosphodiesterase activity, this assay was shown to generate comparable data with reference compounds to an ALPHA-screen assay using a more traditional tyrosyl-oligonucleotide substrate. This served to validate its use as a direct assay for TDP1 activity.⁴⁴

While this paper was in preparation, Schellenberg et al. reported the X-ray structure of the catalytic domain of mouse TDP2 bound to DNA,⁵² alongside a publication from Shi et al.

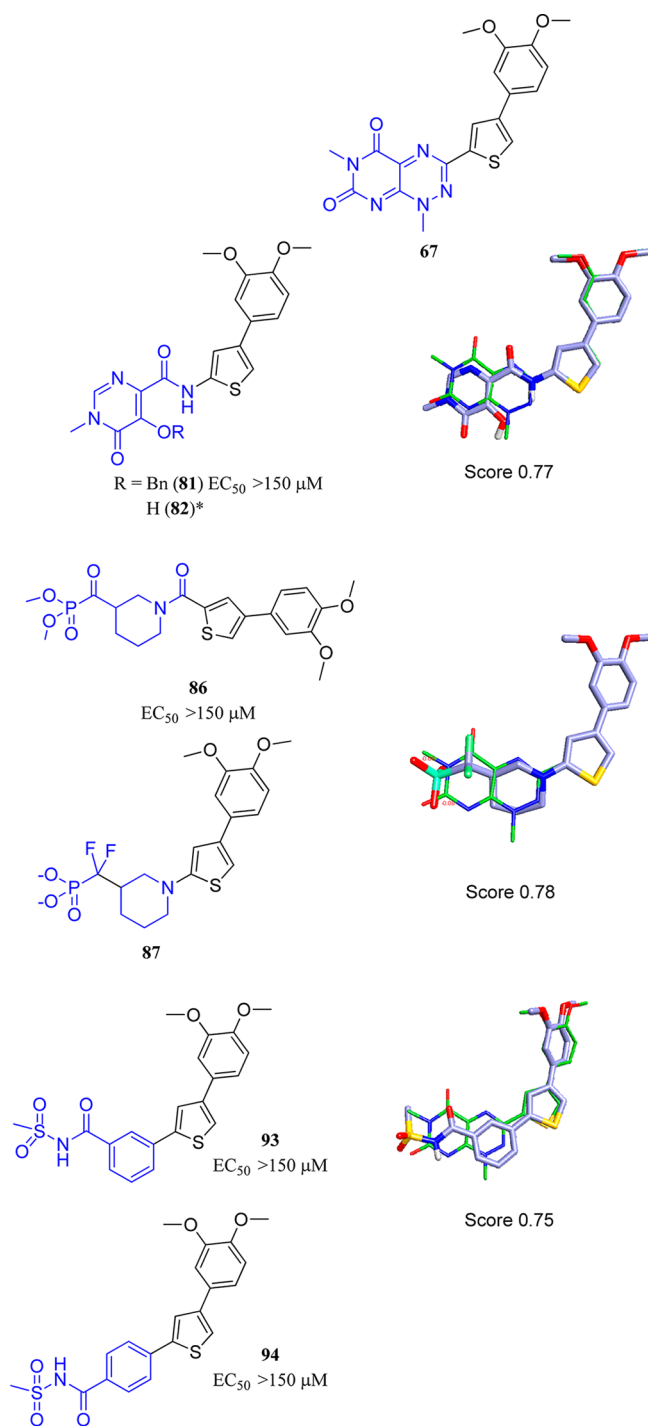


Figure 3. Toxoflavin phosphate mimetics. Putative phosphate mimetics were attached to the thiophene dimethoxyphenyl moiety of **67** via various linkers, aligned using Torch software from Cresset.⁴⁸ This highlights designs most similar to **67** in terms of shape and electrostatic properties. Scores of 0.7 or greater were considered favorable.

detailing both zebrafish and *Caenorhabditis elegans* homologues.⁵³ The Schellenberg disclosure was the first structure of a mammalian TDP2 to be published. Alongside mutational and functional analyses, the structural data supported a single metal ion catalytic mechanism for cleavage of the tyrosyl-DNA adduct. Mouse TDP2 is highly homologous to human TDP2, with the catalytic site being particularly well conserved (Figure

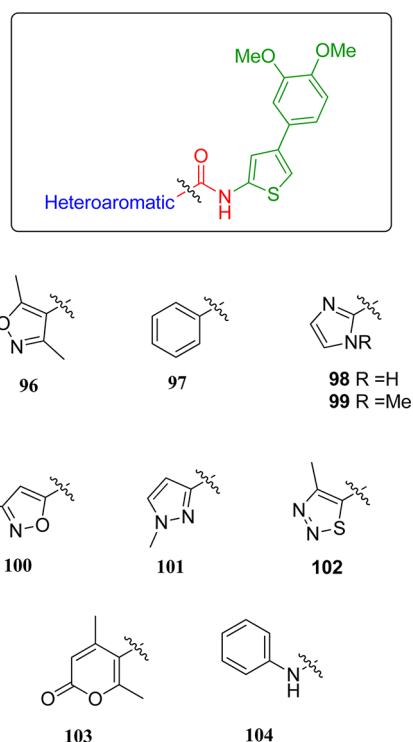


Figure 4. Computationally designed core variations of toxoflavins.

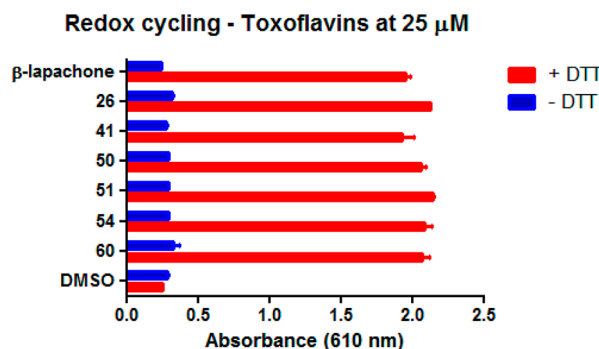


Figure 5. Toxoflavins: hydrogen peroxide generation as an indicator of redox activity. Redox cycling compounds can generate H_2O_2 in the presence of reducing reagents such as DTT, which can in turn oxidize accessible cysteine, tryptophan, methionine, histidine, or selenocysteine residues, resulting in the nonspecific inhibition of enzymatic activity. Compounds were assayed for redox cycling potential by measuring generation of H_2O_2 in the presence and absence of 1 mM DTT. This assay detects H_2O_2 production using a coupled enzymatic assay via the H_2O_2 -dependent horseradish peroxidase (HRP)-mediated oxidation of phenol red and measurement of the subsequent change in absorbance at 610 nm at alkaline pH.⁵¹ The known redox cycling compound β -lapachone was employed as a positive control, and 1% DMSO was used as the negative control for this assay.

10). In order to determine whether the mouse structure was able to yield any insight into the potential binding mode and SAR of the deazaflavin series, docking studies were performed using Glide.⁴⁷ Of the four X-ray structures reported by Schellenberg et al., the structure of the TDP2–DNA reaction product complex (PDB code 4GZ1) was selected as a suitable starting point for docking studies, being a well-resolved (1.5 Å) structure with the catalytic magnesium ion in position. The DNA duplex and solvent were removed prior to docking. A selection of the most active deazaflavin compounds were

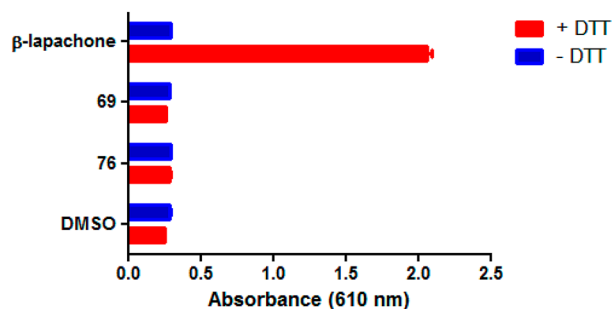
Redox cycling - Toxoflavin deletions at 25 μ M

Figure 6. Toxoflavins deletion compounds: hydrogen peroxide generation as an indicator of redox activity. β -Lapachone was employed as a positive control, and 1% DMSO was used as the negative control for this assay.

docked, with the pyrimidodione ring A represented in both protonated (neutral) and deprotonated (anionic) forms.

Several binding modes were consistently observed for deazaflavin analogues, typified by the pyrimidodione ring binding to the magnesium ion and gaining one or more hydrogen bonding interactions to neighboring phosphate-binding residues. One such binding mode is illustrated in Figure 11. The tricyclic deazaflavin core fits along the shallow floor of the DNA binding site, with the pyrimidodione ring A bound to the magnesium ion and to an “oxyanion hole” involved in 5'-phosphoryl binding (i.e., side chains of His236 and Ser239, mouse TDP2 numbering). In terms of the SAR of the deazaflavin series, N-methylation of ring A, such as in compound 133, was seen to abolish activity, which is consistent with the hypothesis that ring A, possibly in a deprotonated state, forms critical metal and hydrogen-bonding interactions. The R¹ phenyl group, which in its lowest energy conformation is predicted to be oriented orthogonal to the plane of the tricyclic core in a “sailboat” conformation, binds to the hydrophobic wall in the region of Leu315. Although in this model the tetrazole substituent forms no specific interactions, it may be that a degree of protein flexibility will allow direct or water-mediated hydrogen-bonding contacts to polar sites in the region of the hydrophobic wall (e.g., Leu315 backbone, Arg316 side chain) or on the opposite loop (e.g., Thr240, His243). Electron-withdrawing groups on ring C at R³ (e.g., nitrile, 163) may be important for stabilizing the deprotonation of ring A or for enhancing aromatic stacking interactions between ring C and neighboring residues such as Trp307, Phe325, and Arg327 (Figure 11).

While docking studies proved useful for suggesting potential binding modes, it should be borne in mind that the conformation of human TDP2 may not be identical to the available X-ray structures of mouse TDP2, particularly if a degree of induced fit binding to the ligand should arise in the absence of bound DNA.

The solubility and permeability of the deazaflavins were next investigated to triage the selection of compounds for cell assay profiling. The potent methanesulfonamide 147 exhibited good aqueous solubility but low Caco-2 permeability. Compound 147, a close analogue of 157, was less soluble and also displayed high levels of efflux. These DMPK issues may have been attributed to the increased lipophilicity and hence calculated log P^{45} of compound 159 (Table 6). The efflux liability was further investigated by profiling the nitrile and the methanesulfonamide deletion compounds 158 and 146, respectively. Low

permeability and high efflux still remained an issue with the deazaflavins. However, the unsubstituted core 130, while inactive, exhibited good solubility and permeability and reduced efflux, which implied that the poor *in vitro* DMPK properties were not an intrinsic liability of deazaflavins in general. This encouraging result prompted the profiling of further analogues in an attempt to balance potency, solubility and permeability, and lipophilicity (compounds 149, 154, and 160). Unfortunately, the permeability of our TDP2-active elaborated derivatives remained low. However, the potent tetrazole 163 displayed the best balance of potency and physicochemical properties.

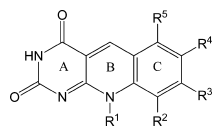
Selectivity for the deazaflavins against TDP1 and APE-1 was maintained in these advanced analogues, and testing additional analogues in the hydrogen peroxide assessment encouragingly reinforced the initial findings for this series of inhibitors as being devoid of a potential redox cycling liability (Figure 12).

CONCLUSION

The toxoflavins were initially identified as potent and selective inhibitors of the TDP2 enzyme. Although there is precedence for the drug-like nature of such compounds, redox activity in the biochemical assay strongly suggested that the SAR from the medicinal chemistry design was not representative of toxoflavin pharmacology against TDP2, and with hindsight, this is consistent with the redox potential of these compounds. Consistent with this conclusion, core deletions, variations, and phosphate mimetics all resulted in the loss of activity. Given the prevalence of these compounds in the medicinal chemistry literature and their common incorporation into screening libraries, we feel it is critically important to raise awareness of this liability in the community and to highlight more widely these scaffolds as demonstrated assay interference compounds. We hope this report will alert others to the issue we have experienced despite apparently clear and rational SAR against our chosen target.

Despite this, a singleton hit from the deazaflavin class of compounds was successfully translated to a potent series with no observed redox liabilities, and significant SAR has been elaborated that is distinct from the toxoflavin series. The deazaflavins were further tested in an orthogonal and more pharmacologically relevant oligonucleotide biochemical assay. In comparison to the chromogenic assay, both the rank order of compound inhibition and potencies were in very good correlation. The robustness of all data were verified by the acceptable standard deviations. There was no evidence of compound precipitation or aggregation in all assay formats. This was also supported by hill slopes approximating unity in all cases. Computational studies based on the close homology mouse TDP2 crystal structure provided possible explanations for the observed SAR, and therefore potential mechanism of inhibition by the deazaflavin series. However, generally low permeability in the Caco-2 assay prevented further progression of this series. Nevertheless, 163 exhibited the most balanced profile of all the deazaflavins synthesized and therefore may offer a potential candidate for investigating the proof of mechanism of TDP2 inhibition in appropriate cell lines, permeabilized cell systems, or cell lysates. As such, this work offers useful preliminary tool compounds for the exploration of the novel biological effects of TDP2 inhibition and may serve as a starting point for the elaboration of more advanced, cell-penetrant derivatives in due course. Moreover, should these agents confirm a critical role of TDP2 in the reversal of

Table 4. Deazaflavins SAR



compound	R ¹	R ²	R ³	R ⁴	R ⁵	EC ₅₀ (μM) ^a
128	phenyl	H	Cl	H	H	7.36(0.24)
129	phenyl	H	H	H	H	>30
130	methyl	H	H	H	H	<i>b</i>
131	benzyl	H	Cl	H	H	>30
132	4-tolyl	H	Cl	H	H	>30
133-N-methyl pyrimidodione	phenyl	H	Cl	H	H	>30
134	phenyl	Cl	H	H	H	>10
135	phenyl	H	H	Cl	H	>10
136	phenyl	H	H	H	Cl	>10
137	methyl	H	Cl	H	H	>30
138	cyclopropyl	H	Cl	H	H	>30
139	cyclohexyl	H	Cl	H	H	>30
140	4-piperidyl	H	Cl	H	H	>30
141	4-hydroxyphenyl	H	Cl	H	H	1.66(0.45)
142	4-methoxyphenyl	H	Cl	H	H	>30
143	3-hydroxyphenyl	H	Cl	H	H	0.48(0.04)
144	2-hydroxyphenyl	H	Cl	H	H	>30
145	phenyl	H	CF ₃	H	H	2.87(1.62)
146	phenyl	H	CN	H	H	0.50(0)
147	3-hydroxyphenyl	H	CN	H	H	0.05(0)
148	4-hydroxyphenyl	H	CN	H	H	0.09(0.01)
149	3-(hydroxymethyl)phenyl	H	CN	H	H	0.25(0.01)
150	3-methoxyphenyl	H	CN	H	H	0.47(0.44)
151	4-methoxyphenyl	H	CN	H	H	1.04(0.20)
152	3-hydroxy-4-methoxyphenyl	H	CN	H	H	0.32(0.18)
153	3-fluorophenyl	H	CN	H	H	3.39(1.71)
154	4-bromophenyl	H	CN	H	H	2.74(3.66)
155	3-aminophenyl	H	CN	H	H	0.09(0.03)
156	3-phenylacetamide	H	CN	H	H	0.72(0.11)
157	3-phenylmethanesulfonamide	H	CN	H	H	0.03(0.01)
158	3-phenylmethanesulfonamide	H	H	H	H	4.66(1.32)
159	3-phenylmethanesulfonamide	H	H	Cl	H	1.37(0.30)
160	3-benzenesulfonamide	H	CN	H	H	0.29(0.06)
161	1H-indazol-6-yl	H	CN	H	H	0.64(0.27)
162	1H-indazol-4-yl	H	CN	H	H	0.37(0.07)
163	3-(1H-tetrazol-5-yl)phenyl	H	CN	H	H	0.04(0)

^aValues stated are a geometric mean of at least two independent determinations with standard deviations given in parentheses. The inhibition values were expressed as EC₅₀ values rather than IC₅₀ values, as all inhibitory compounds tested showed a maximum inhibition of approximately 75%, reaching a plateau at this level (see Figure 8 for a typical curve). All inhibitory compounds show hill slopes approximating unity. Dose response curves of all active deazaflavins can be found in the Supporting Information. ^b10% inhibition at 50 μM.

resistance to commonly used chemotherapeutic agents, such permeable derivatives may have the potential to deliver considerable clinical utility.

EXPERIMENTAL SECTION

General Methods. All reagents obtained from commercial sources were used without further purification. Anhydrous solvents were obtained from the Sigma-Aldrich Chemical Co. Ltd. or Fisher Chemicals Ltd. and used without further drying. Solutions containing products were either passed through a hydrophobic frit or dried over anhydrous MgSO₄ or Na₂SO₄ and filtered prior to evaporation of the solvent under reduced pressure. Thin layer chromatography (TLC) was conducted with 5 cm × 10 cm plates coated with Merck type 60 F254 silica gel to a thickness of 0.25 mm. Chromatography was performed on Biotage SNAP HP-Sil cartridges using a CombiFlash Companion machine. Proton (¹H) and carbon (¹³C) NMR spectra

were recorded on a 300 MHz Bruker spectrometer at ambient temperature. Solutions were typically prepared in either deuteriochloroform (CDCl₃) or deuterated dimethylsulfoxide (DMSO-*d*₆) with chemical shifts referenced to deuterated solvent as an internal standard. ¹H NMR data are reported indicating the chemical shift (δ), the multiplicity (s, singlet; d, doublet; t, triplet; q, quartet; m, multiplet; br, broad; dd, doublet of doublets, etc.), the coupling constant (*J*) in Hz, and the integration (e.g., 1H). Deuterated solvents were obtained from the Sigma-Aldrich Chemical Co., Goss, or Fluorochem. HRMS results were obtained on a Waters QToF Micro instrument, using positive and negative polarity electrospray with sodium formate as standard calibrant. LC-MS spectra with UV detection were recorded on a Waters Acquity UPLC. Mass spectrometry was performed on a Waters Acquity SQD quadrupole spectrometer running in dual ES+ and ES- mode. High pH runs were conducted at pH 10, and low pH runs were conducted at pH 3, with a run time of 2 min. The column temperature was 40 °C, and the flow

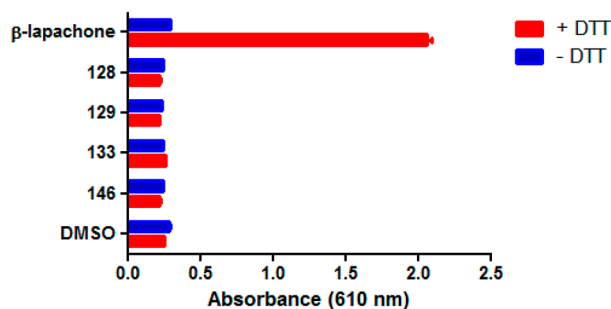
Redox cycling - Deazaflavin hit confirmation at 25 μM 

Figure 7. Deazaflavins early SAR compounds: hydrogen peroxide generation as an indicator of redox activity. β -Lapachone was employed as a positive control, and 1% DMSO was used as the negative control for this assay.

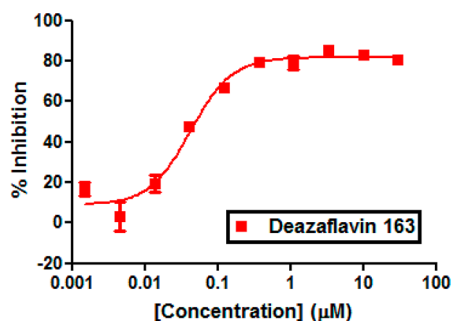


Figure 8. Dose–response curve of a representative deazaflavin 163.

rate was 0.6 mL/min. Further details, including solvent gradients, are given in the Supporting Information. Details of the preparative HPLC instrument and the solvent gradient used to purify compounds are also given in the Supporting Information. All compounds were $\geq 95\%$ purity as determined by examination of both the LC-MS and ^1H NMR spectra unless otherwise indicated. Where Cl or Br were present, expected isotopic distribution patterns were observed.

(3,4-Dimethoxy-phenyl)-thiophen-2-ylamine was purchased from Princeton BioMolecular Research Inc. Compound 79 was purchased from Sigma-Aldrich Company Ltd. Compounds 53, 128, 129, and 131–133 were purchased from InterBioScreen Ltd., Moscow, Russia, and used as received.

Compound 69 can be commercially sourced from Princeton BioMolecular Research, Inc. Compound 54 can be commercially sourced from Ambinter Stock Screening Collection.

3-(4-Chlorophenyl)-1,6-dimethyl-pyrimido[5,4-e][1,2,4]triazine-5,7-dione, 24.²⁴ In adaptation of the literature procedure,²¹ a suspension of 2 (480 mg, 1.64 mmol) in AcOH (25 mL) at ambient temperature was treated with a solution of sodium nitrite (170 mg, 2.46 mmol) in water (2.5 mL) and stirred for 18 h. The reaction mixture was diluted with Et₂O (50 mL), and the flask was cooled in an ice bath and scratched. After the mixture was stirred for 30 min, the precipitate was collected by filtration and washed with Et₂O (2 \times 10 mL). The solid was dried to afford a 7:3 mixture of the product 24/*N*-oxide (at *N*-4) as a bright yellow solid, 419 mg. A 200 mg sample of this was suspended in EtOH (18 mL) and treated with a solution of 1,4-bis(sulfanyl)butane-2,3-diol (145 mg, 0.94 mmol) (5 equiv with respect to the amount of *N*-oxide) in water (1.8 mL). The dark orange mixture was heated to 50 $^\circ\text{C}$ for 1 h and then allowed to cool to ambient temperature. The precipitate was collected by filtration, washed with EtOH (2 \times 5 mL), and dried to afford 24 (orange solid, 125 mg, 25%); LC-MS (high pH) 0.97 min, *m/z* 304.5 [M + H]⁺, 100% purity.

1,6-Dimethyl-3-phenyl-pyrimido[5,4-e][1,2,4]triazine-5,7-dione, 25.³⁴ Compound 25 was prepared in a manner analogous to that for

Table 5. Oligonucleotide assay versus NPPP assay

compound	oligonucleotide assay IC ₅₀ (μM) ^a	NPPP assay EC ₅₀ (μM) ^{a,b}
54 ^c	1.51(0.03)	0.51(0.23)
129	>30	>30
130	>30	>30
131	>30	>30
132	>30	>30
137	>30	>30
139	>30	>30
140	>30	>30
141	7.04(1.36)	1.66(0.45)
142	>30	>30
143	2.41(0.49)	0.48(0.04)
144	27.48(0.74)	>30
145	12.96(0.62)	2.87(1.62)
146	3.71(0.07)	0.50(0)
147	0.52(0.11)	0.05(0)
148	1.45(0.12)	0.09(0.01)
152	2.15(0.46)	0.32(0.18)
154	12.51(1.88)	2.74(3.66)
157	0.64(0.29)	0.03(0.01)
161	3.63(0.70)	0.64(0.27)
162	3.82(1.04)	0.37(0.07)
163	0.59(0.09)	0.04(0)

^aValues stated are a geometric mean of at least two independent determinations with standard deviations given in parentheses, and all inhibitory compounds show hill slopes approximating unity. ^bThe inhibition values were expressed as EC₅₀ values rather than IC₅₀ values because all inhibitory compounds tested showed a maximum inhibition of 75%, reaching a plateau at this level. ^cToxoflavin 54 was tested to show oligo assay robustness against two distinct chemical series.

24 (orange solid, 223 mg, 53%); LC-MS (high pH) 0.87 min, *m/z* 270.5 [M + H]⁺, 100% purity.

3-(4-Ethylphenyl)-1,6-dimethyl-pyrimido[5,4-e][1,2,4]triazine-5,7-dione, 26. Compound 26 was prepared in a manner analogous to that for 24 (orange solid, 160 mg, 31%). ^1H NMR (CDCl₃): δ 8.23 (d, *J* = 8.3 Hz, 2H), 7.3 (d, *J* = 8.3 Hz, 2H), 4.23 (s, 3H), 3.53 (s, 3H), 2.74 (q, *J* = 7.6 Hz, 2H), 1.29 (t, *J* = 7.6 Hz, 3H).

1,6-Dimethyl-3-[4-(trifluoromethyl)phenyl]pyrimido[5,4-e][1,2,4]triazine-5,7-dione, 27. Compound 27 was prepared in a manner analogous to that for 24 (yellow solid, 26 mg, 5%); LC-MS (high pH) 1.03 min, *m/z* 338.5 [M + H]⁺, 100% purity.

1,6-Dimethyl-3-[4-(trifluoromethoxy)phenyl]pyrimido[5,4-e][1,2,4]triazine-5,7-dione, 28. Compound 28 was prepared in a manner analogous to that for 24 (orange solid, 36 mg, 7%). ^1H NMR (CDCl₃): δ 8.37 (d, *J* = 8.7 Hz, 2H), 7.36 (d, *J* = 8.7 Hz, 2H), 4.24 (s, 3H), 3.53 (s, 3H).

1,6-Dimethyl-3-(*p*-tolyl)pyrimido[5,4-e][1,2,4]triazine-5,7-dione, 29.²⁴ Compound 29 was prepared in a manner analogous to that for 24 (orange solid, 549 mg, 59%); LC-MS (high pH) 0.96 min, *m/z* 284.5 [M + H]⁺, 100% purity.

1,6-Dimethyl-3-(*m*-tolyl)pyrimido[5,4-e][1,2,4]triazine-5,7-dione, 30. Compound 30 was prepared in a manner analogous to that for 24 (yellow solid, 297 mg, 73%). ^1H NMR (CDCl₃): δ 8.08–8.14 (m, 2H), 7.33–7.44 (m, 2H), 4.24 (s, 3H), 3.53 (s, 3H), 2.46 (s, 3H).

1,6-Dimethyl-3-(*o*-tolyl)pyrimido[5,4-e][1,2,4]triazine-5,7-dione, 31. Compound 31 was prepared in a manner analogous to that for 24 (orange solid, 133 mg, 32%); LC-MS (high pH) 0.91 min, *m/z* 284.5 [M + H]⁺, 100% purity.

3-(4-Ethylphenyl)-6-methyl-8H-pyrimido[5,4-e][1,2,4]triazine-5,7-dione, 69, and 1-Ethyl-3-(4-ethylphenyl)-6-methyl-pyrimido[5,4-e][1,2,4]triazine-5,7-dione, 38. A suspension of the commercially available 32 in AcOH (15 mL) was treated with a solution of sodium nitrite (93.2 mg, 1.35 mmol) in water (2 mL) at ambient temperature. The reaction was stirred for 16 h. Et₂O (100 mL) was added, and the

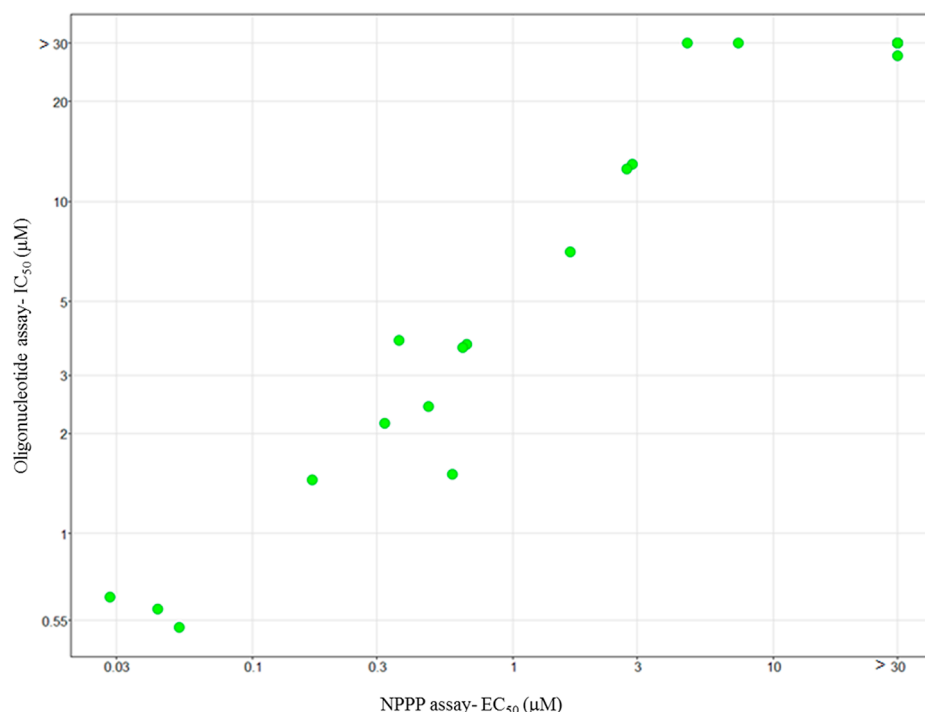


Figure 9. Correlation plot of compound inhibition in the two complementary biochemical assays. R^2 of correlation = 0.97.

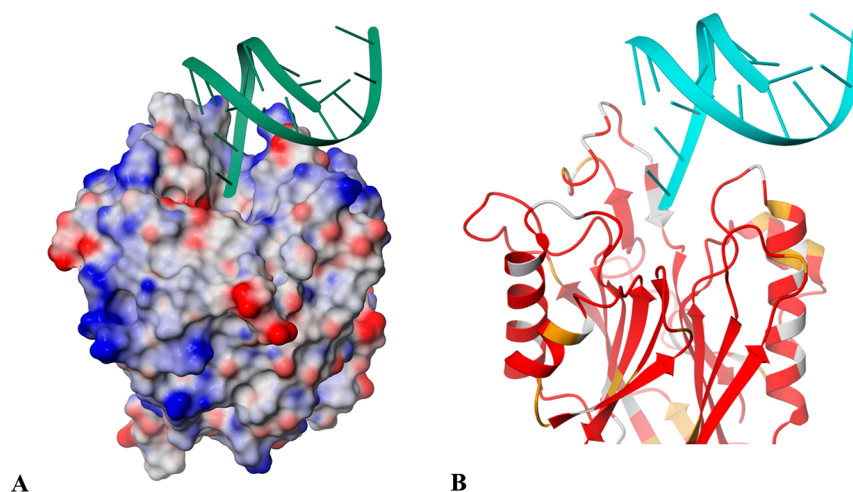


Figure 10. Comparison of mouse and human TDP2 active site sequence homology. The X-ray structure of the mouse TDP2/DNA complex (PDB 4GZ1).⁵² (A) Protein solvent-accessible surface colored by electrostatic potential. (B) Detail of the protein/DNA interface, with the protein backbone colored in terms of homology to human TDP2 (red, identical residue; orange, similar; gray, dissimilar). Figures prepared using Maestro.⁴⁷

mixture was cooled in an ice bath. After the mixture was stirred for 30 min, the solids were collected by filtration and washed with Et₂O (2 × 20 mL) to afford a 3:2 mixture of **38**/**68** *N*-oxide (at *N*-4) as an orange solid, 314 mg. A suspension of the mixture in EtOH (20 mL) was treated with a solution of 1,4-bis(sulfanyl)butane-2,3-diol (75.8 mg, 0.49 mmol) in water (2 mL) and heated to reflux for 16 h. The cooled reaction mixture was diluted with Et₂O, and the resulting precipitate was collected by filtration, washed with diethyl ether, and dried to give **69** (orange solid, 16 mg, 11%). ¹H NMR (DMSO-*d*₆): δ 8.33 (d, *J* = 8.0 Hz, 2H), 7.45 (d, *J* = 8.0 Hz, 2H), 3.30 (s, 3H), 2.72 (q, *J* = 7.3 Hz, 2H), 1.25 (t, *J* = 7.5 Hz, 3H). The filtrate was concentrated and purified by preparative HPLC at high pH to give **38** (yellow solid, 1.97 mg, 1%). ¹H NMR (CDCl₃): δ 8.16 (d, *J* = 8.2 Hz, 2H), 7.28 (d, *J* = 8.2 Hz, 2H), 4.61 (q, *J* = 7.3 Hz, 2H), 3.45 (s, 3H), 2.67 (q, *J* = 7.5 Hz, 2H), 1.54 (t, *J* = 7.2 Hz, 3H), 1.22 (t, *J* = 7.7 Hz, 3H).

1-(Cyclopropylmethyl)-3-(4-ethylphenyl)-6-methyl-pyrimido[5,4-*e*][1,2,4]-triazine-5,7-dione, **39**. Compound **39** was prepared in a manner

analogous to that for **41** (orange solid, 841 mg, 27%). ¹H NMR (DMSO-*d*₆): δ 8.09 (d, *J* = 8.2 Hz, 2H), 7.43 (d, *J* = 8.2 Hz, 2H), 4.57–4.66 (m, 1H), 2.70 (q, *J* = 7.6 Hz, 2H), 1.41–1.48 (m, 2H), 1.27–1.34 (m, 2H), 1.22 (t, *J* = 7.6 Hz, 3H).

3-(4-Ethylphenyl)-6-methyl-1-propyl-pyrimido[5,4-*e*][1,2,4]-triazine-5,7-dione, **40**. Compound **40** was prepared in a manner analogous to that for **41** (orange solid, 201 mg, 27%). ¹H NMR (DMSO-*d*₆): δ 8.11 (d, *J* = 8.2 Hz, 2H), 7.43 (d, *J* = 8.2 Hz, 2H), 4.33–4.46 (m, 2H), 2.70 (q, *J* = 7.6 Hz, 2H), 1.87–2.01 (m, 2H), 1.23 (t, *J* = 7.6 Hz, 3H), 0.99 (t, *J* = 7.4 Hz, 3H).

1-(Cyclopropylmethyl)-3-(4-ethylphenyl)-6-methyl-pyrimido[5,4-*e*][1,2,4]-triazine-5,7-dione, **41**. To a solution of **35** (1.0 g, 3.06 mmol) in AcOH (40 mL) and water (4 mL) at 5 °C under nitrogen was added NaNO₂ (296 mg, 4.29 mmol), and the resulting mixture was stirred at 5 °C for 10 min before being warmed to ambient temperature and stirred for a further 4 h. LCMS analysis of the reaction mixture showed a 1:1 mixture of **41**/*N*-oxide (at *N*-4). 1,4-

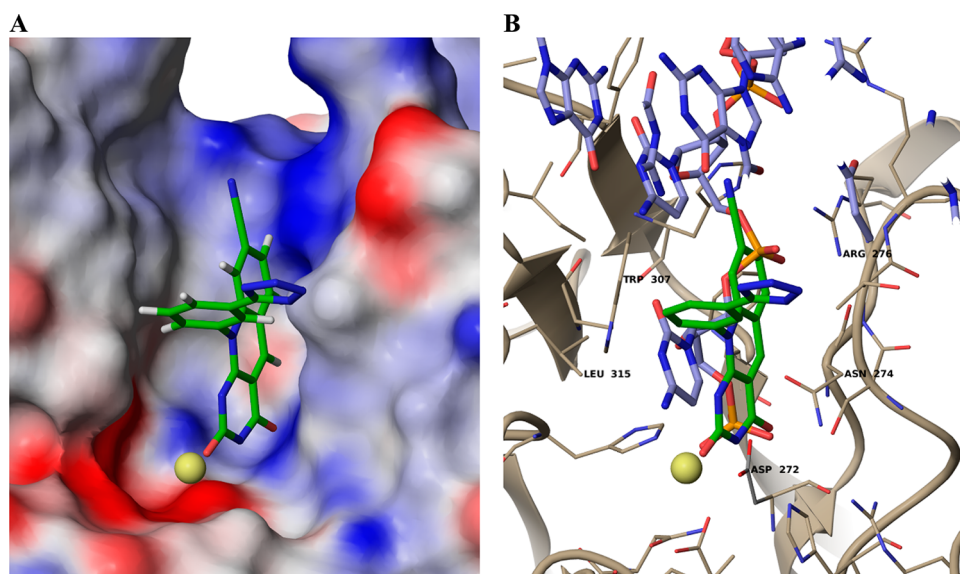


Figure 11. Postulated binding mode of deazaflavin **163**. Detail of a typical predicted binding mode for deazaflavin compound **163** ($R^1 = 3-(1H\text{-tetrazol-5-yl})\text{phenyl}$, $R^3 = \text{CN}$) docked to the X-ray structure of mouse TDP2. (A) Protein solvent-accessible surface colored by electrostatic potential, with the magnesium ion shown as a yellow sphere. (B) Same docked pose of compound **163** compared with the binding mode of the DNA duplex in the original X-ray structure (thick stick, purple carbon atoms, orange phosphorus atoms). Figures prepared using Maestro.⁴⁷

Table 6. Deazaflavins in Vitro DMPK

compound	xLogP	aqueous solubility ^a (μM)	$P_{a \rightarrow b}$ ^b ($10^{-6} \text{ cm s}^{-1}$)	$\frac{P_{b \rightarrow a}}{P_{a \rightarrow b}}$
130	1.04	100	12.10	3.5
146	2.60	100	0.44	11.4
149	1.97	100	0.30	2.6
154	3.40	1–10	<i>c</i>	<i>d</i>
157	1.49	30–100	0.16	2.4
158	1.77	1–65	0.41	7.5
159	2.39	10–65	0.25	13.7
160	1.19	100	0.25	2.0
163	2.57	100	1.34	0.1

^aTurbidimetric aqueous solubility: concentration of test compound that produces an increase in absorbance above 1% DMSO in buffer.

^b $P_{a \rightarrow b}$ is the permeability when applied to the apical side, while $P_{b \rightarrow a}$ is the permeability when applied to the basolateral side in a Caco-2 membrane assay. The ratio of these two values is a measure of Pgp efflux, while the $P_{a \rightarrow b}$ value is a measure of permeability.

^cUndetectable. ^dNot applicable.

Redox cycling - Deazaflavins hit to lead at 25 μM

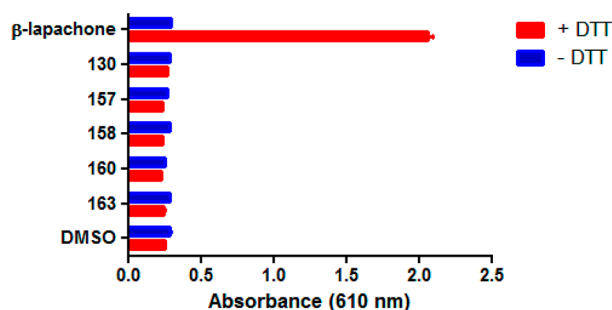


Figure 12. Deazaflavins hit to lead—hydrogen peroxide generation as an indicator of redox activity. β -Lapachone was employed as a positive control, and 1% DMSO was used as the negative control for this assay.

Bis(sulfanyl)butane-2,3-diol (473 mg, 3.06 mmol) was added, and the resulting mixture was stirred for 1 h. The mixture was concentrated

under vacuum, and the residue was suspended in EtOH (20 mL) and stirred for 16 h. The solid was collected by filtration and washed with EtOH ($2 \times 10 \text{ mL}$) and preadsorbed onto silica. The material was purified by flash column chromatography, eluting with a gradient of DCM to 2% MeOH/DCM to afford **41** (orange solid, 600 mg, 58%). ¹H NMR (DMSO- d_6): δ 8.15 (d, $J = 8.2 \text{ Hz}$, 2H), 7.47 (d, $J = 8.2 \text{ Hz}$, 2H), 4.35 (d, $J = 7.0 \text{ Hz}$, 2H), 3.35 (s, 3H), 2.73 (q, $J = 7.6 \text{ Hz}$, 2H), 1.43–1.55 (m, 1H), 1.25 (t, $J = 7.6 \text{ Hz}$, 3H), 0.55–0.68 (m, 4H).

3-(4-Ethylphenyl)-6-methyl-1-phenyl-pyrimido[5,4-*e*][1,2,4]-triazine-5,7-dione, 42. Compound **42** was prepared in a manner analogous to that for **41**. The product **42** and *N*-oxide (at *N*-4) were isolated crude, after trituration with Et₂O, as an approximate 8:2 mixture before the final step reduction was carried out in refluxing ethanol for 1 h. The crude product was purified by preparative low pH HPLC to give **42** (orange solid, 8.8 mg, 4%). ¹H NMR (CDCl₃): δ 8.20 (d, $J = 8.2 \text{ Hz}$, 2H), 7.72–7.88 (m, 2H), 7.43–7.59 (m, 3H), 7.28 (d, $J = 8.2 \text{ Hz}$, 2H), 3.47 (s, 3H), 2.68 (q, $J = 7.6 \text{ Hz}$, 2H), 1.24 (t, $J = 7.6 \text{ Hz}$, 3H).

1-Benzyl-3-(4-ethylphenyl)-6-methyl-pyrimido[5,4-*e*][1,2,4]-triazine-5,7-dione, 43.⁵⁴ To a solution of **69** (80 mg, 0.28 mmol) in 1,4-dioxane (10 mL) was added K₂CO₃ (78 mg, 0.56 mmol) followed by benzyl bromide (0.1 mL, 0.85 mmol). The reaction mixture was heated at reflux for 5 h and then concentrated under vacuum. The residue was recrystallized from EtOH to afford **43** (orange solid, 11 mg, 10%); LC-MS (high pH) 1.38–1.40 min, m/z 374.4 [M + H]⁺, 100% purity.

3-(4-Ethylphenyl)-1-methyl-pyrimido[5,4-*e*][1,2,4]triazine-5,7-dione, 50. Compound **50** was prepared in a manner analogous to that for **52** (orange solid, 140 mg, 67%). ¹H NMR (CDCl₃): δ 8.52 (br. s, 1H), 8.21 (d, $J = 8.6 \text{ Hz}$, 2H), 7.34 (d, $J = 8.6 \text{ Hz}$, 2H), 4.24 (s, 3H), 2.74 (q, $J = 7.7 \text{ Hz}$, 2H), 1.29 (t, $J = 7.7 \text{ Hz}$, 3H).

3-(4-Ethylphenyl)-1-methyl-6-phenyl-pyrimido[5,4-*e*][1,2,4]-triazine-5,7-dione, 51. Compound **51** was prepared in a manner analogous to that for **52** (orange solid, 60 mg, 39%). ¹H NMR (CDCl₃): δ 8.23 (d, $J = 8.2 \text{ Hz}$, 2H), 7.42–7.57 (m, 4H), 7.28–7.38 (m, 3H), 4.28 (s, 3H), 2.74 (q, $J = 7.6 \text{ Hz}$, 2H), 1.29 (t, $J = 7.6 \text{ Hz}$, 3H).

6-Benzyl-3-(4-ethylphenyl)-1-methyl-pyrimido[5,4-*e*][1,2,4]-triazine-5,7-dione, 52. In an adaptation of the literature procedure,²⁴ to a mixture of **49** (100 mg, 0.28 mmol) in AcOH (5 mL) and water (0.5 mL) at 5 °C under an atmosphere of nitrogen was added NaNO₂ (29 mg, 0.41 mmol), and the resulting mixture was stirred at 5 °C for 10 min before being warmed to ambient temperature and stirred for a

further 16 h. LC-MS analysis indicated a 4:1 mixture of **52**/*N*-oxide (at *N*-4). The reaction mixture was concentrated, and the residue was dissolved in a 10:1 (v/v) mixture of EtOH/water (10 mL). 1,4-Bis(sulfanyl)butane-2,3-diol (85 mg, 0.55 mmol) was added, and the resulting mixture was stirred for 10 min. The mixture darkened considerably, and a solid formed, which was collected by filtration and washed with EtOH (2 × 10 mL). The crude material was preadsorbed onto silica and purified by flash column chromatography, eluting with a gradient of DCM to 5% MeOH/DCM to afford **52** (orange solid, 50 mg, 49%). ¹H NMR (CDCl₃): δ 8.20 (d, *J* = 8.4 Hz, 2H), 7.56–7.61 (m, 2H), 7.24–7.35 (m, 5H), 5.28 (br. s, 2H), 4.21 (s, 3H), 2.73 (q, *J* = 7.6 Hz, 2H), 1.28 (t, *J* = 7.6 Hz, 3H).

1,6-Dimethyl-3-propyl-pyrimido[5,4-*e*][1,2,4]triazine-5,7-dione, 54. Compound **54** was prepared in a manner analogous to that for **24**, but in this example, the reaction mixture was concentrated and purified by flash column chromatography, eluting with a gradient of DCM to 5% MeOH/DCM (yellow solid, 12 mg, 3%); LC-MS (high pH) 0.74 min, *m/z* 236.5 [M + H]⁺, >95% purity.

3-Cyclopropyl-1,6-dimethyl-pyrimido[5,4-*e*][1,2,4]triazine-5,7-dione, 55. Compound **55** was prepared in a manner analogous to that for **24** using crude hydrazone, but in this example, the reaction mixture was concentrated and purified by flash column chromatography, eluting with a gradient of DCM to 5% MeOH/DCM, followed by trituration with diethyl ether (yellow solid, 142 mg, 32% yield from chlorouracil **1**); LC-MS (high pH) 0.64 min, *m/z* 234.5 [M + H]⁺, >95% purity.

3-Cyclopentyl-1,6-dimethyl-pyrimido[5,4-*e*][1,2,4]triazine-5,7-dione, 56. Compound **56** was prepared in a manner analogous to that for **24**, but in this example, the reaction mixture was concentrated and purified by flash column chromatography, eluting with a gradient of DCM to 5% MeOH/DCM (yellow solid, 66 mg, 49%). ¹H NMR (CDCl₃): δ 4.12 (s, 3H), 3.49 (s, 3H), 3.34–3.46 (m, 1H), 1.69–2.18 (m, 8H).

3-Cyclohexyl-1,6-dimethyl-pyrimido[5,4-*e*][1,2,4]triazine-5,7-dione, 57.⁵⁵ Compound **57** was prepared in a manner analogous to that for **24**, but in this example, the reaction mixture was purified by preparative HPLC (yellow solid, 2 mg, 1%); LC-MS (high pH) 0.96 min, *m/z* 276.5 [M + H]⁺, >95% purity.

1,6-Dimethyl-3-tetrahydropyran-4-yl-pyrimido[5,4-*e*][1,2,4]triazine-5,7-dione, 58. Compound **58** was prepared in a manner analogous to that for **24**, but in this example, the reaction mixture was concentrated and purified by flash column chromatography, eluting with a gradient of DCM to 5% MeOH/DCM (yellow solid, 20 mg, 4%). ¹H NMR (CDCl₃): δ 4.13 (s, 3H), 4.06–4.13 (m, 2H), 3.49–3.58 (m, 2H), 3.49 (s, 3H), 3.17–3.28 (m, 1H), 1.85–2.06 (m, 4H).

3-Benzyl-1,6-dimethyl-pyrimido[5,4-*e*][1,2,4]triazine-5,7-dione, 59.⁵⁵ Compound **59** was prepared in a manner analogous to that for **24** (brown solid, 47 mg, 19%); LC-MS (high pH) 0.87 min, *m/z* 284.5 [M + H]⁺, >95% purity.

1,6-Dimethyl-3-phenethyl-pyrimido[5,4-*e*][1,2,4]triazine-5,7-dione, 60.⁵⁵ Compound **60** was prepared in a manner analogous to that for **24** (yellow solid, 29 mg, 8%); LC-MS (high pH) 0.92 min, *m/z* 298.5 [M + H]⁺, >95% purity.

1,6-Dimethyl-3-thiazol-4-yl-pyrimido[5,4-*e*][1,2,4]triazine-5,7-dione, 63. Compound **63** was prepared in a manner analogous to that for **24**, but in this example, the collected solid was purified by trituration with 10% MeOH/DCM (orange solid, 11 mg, 3%). ¹H NMR (DMSO-*d*₆): δ 9.29 (d, *J* = 1.9 Hz, 1H), 8.53 (d, *J* = 1.9 Hz, 1H), 4.03 (s, 3H), 3.28 (s, 3H).

1,6-Dimethyl-3-(4-methyl-2-thienyl)pyrimido[5,4-*e*][1,2,4]triazine-5,7-dione, 64. Compound **64** was prepared in a manner analogous to that for **24** (orange solid, 207 mg, 54%). ¹H NMR (CDCl₃): δ 7.85 (d, *J* = 1.5 Hz, 1H), 7.12–7.14 (m, 1H), 4.16 (s, 3H), 3.51 (s, 3H), 2.31 (m, 3H).

1,6-Dimethyl-3-(4-phenyl-2-thienyl)pyrimido[5,4-*e*][1,2,4]triazine-5,7-dione, 66. Compound **66** was prepared in a manner analogous to that for **24**, but in this example, the collected solid was purified by trituration with DCM (red solid, 14 mg, 11%). ¹H NMR (CDCl₃): δ 8.30 (d, *J* = 1.5 Hz, 1H), 7.62–7.67 (m, 3H), 7.40–7.47 (m, 2H), 7.35 (tt, *J* = 7.3, 1.3 Hz, 1H), 4.19 (s, 3H), 3.52 (s, 3H).

3-[4-(3,4-Dimethoxyphenyl)-2-thienyl]-1,6-dimethyl-pyrimido[5,4-*e*][1,2,4]triazine-5,7-dione, 67. Compound **67** was prepared in a manner analogous to that for **24** (purple solid, 128 mg, 38%). ¹H NMR (CDCl₃): δ 8.25 (d, *J* = 1.5 Hz, 1H), 7.56 (d, *J* = 1.5 Hz, 1H), 7.20 (dd, *J* = 8.2, 2.2 Hz, 1H), 7.12 (d, *J* = 2.2 Hz, 1H), 6.93 (d, *J* = 8.2 Hz, 1H), 4.20 (s, 3H), 3.98 (s, 3H), 3.93 (s, 3H), 3.52 (s, 3H).

1-Ethyl-3-(4-ethylphenyl)-6-methyl-pyrimido[4,5-*c*]pyridazine-5,7-dione, 70. Compound **70** was prepared according to the literature²⁴ by reaction of the hydrazone intermediate **32** with the commercially available 2-bromo-1-(4-ethylphenyl)ethanone to furnish the product **70** (orange solid, 3.1 mg, 0.6% yield). ¹H NMR (CDCl₃): δ 8.58 (s, 1H), 7.79 (d, *J* = 8.6 Hz, 2H), 7.30 (d, *J* = 8.6 Hz, 2H), 4.70 (q, *J* = 6.7 Hz, 2H), 2.67 (q, *J* = 7.7 Hz, 2H), 1.51 (t, *J* = 7.2 Hz, 3H), 1.11–1.25 (m, 6H).

6-(4-Ethylphenyl)-3,8-dimethyl-pteridine-2,4-dione, 73. Compound **73** was prepared according to the literature,²⁶ by reaction of the intermediate hydrazone **72** with the 6-amino-5-[(*E*)-(4-ethylphenyl)methyleneamino]-1,3-dimethyl-pyrimidine-2,4-dione **71** to afford the product **73** (cream solid, 22.9 mg, 2% yield). ¹H NMR (DMSO-*d*₆): δ 9.37 (s, 1H), 8.10 (d, *J* = 7.8 Hz, 2H), 7.41 (d, *J* = 7.8 Hz, 2H), 3.36 (s, 3H), 3.32 (s, 3H), 2.69 (q, *J* = 7.7 Hz, 2H), 1.24 (t, *J* = 7.7 Hz, 3H).

7-Amino-1-methyl-3-(4-methyl-2-thienyl)pyrimido[5,4-*e*][1,2,4]triazin-5-one, 77. A suspension of **76** (384 mg, 1.46 mmol) in AcOH (14 mL) was treated at ambient temperature with a solution of NaNO₂ (151 mg, 2.19 mmol) in water (1.4 mL). After 40 min, a further 1 equiv of NaNO₂ was added, and the mixture was stirred for an additional 4 h, then cooled to 0 °C and diluted with diethyl ether (30 mL). The precipitated solid was collected by filtration, washed with diethyl ether (2 × 5 mL), and dried to give a red/brown solid, 394 mg as a 1:21 mixture of **77**/*N*-oxide (at *N*-4). This was taken up in EtOH (39 mL), treated with a solution of 1,4-bis(sulfanyl)butane-2,3-diol (528 mg, 3.42 mmol) in water (3.9 mL), and heated to 50 °C for 2 h. The reaction mixture was cooled to ambient temperature, and solids were collected by filtration and washed with EtOH (2 × 5 mL). The filtrate was concentrated to give a red solid, which was preadsorbed onto silica and purified, eluting with a gradient of DCM to 40% MeOH/DCM to afford **77** (orange solid, 10 mg, 3%). ¹H NMR (DMSO-*d*₆): δ 7.63–7.72 (m, 3H), 7.38–7.41 (m, 1H), 3.96 (s, 3H), 2.27 (s, 3H).

7-Amino-1-methyl-3-phenyl-4aH-pyrimido[4,5-*c*]pyridazine-4,5-dione, 78.²⁷ A suspension of **75** (500 mg, 3.22 mmol) in EtOH (25 mL) and water (25 mL) was heated to reflux and treated with ethyl phenylglyoxylate (0.77 mL, 4.83 mmol) in one portion. The reaction mixture was heated at reflux for 22 h, then filtered hot, and the collected solids were washed with 1:1 EtOH/water (2 × 3 mL) and dried to give **78** (pale brown solid, 276 mg, 32%); LC-MS (high pH) 0.70 min, *m/z* 270.5 [M + H]⁺, 100% purity.

5-Benzyloxy-N-[4-(3,4-dimethoxyphenyl)-2-thienyl]-1-methyl-6-oxo-pyrimidine-4-carboxamide, 81. To a solution of 5-benzyloxy-1-methyl-6-oxo-pyrimidine-4-carboxylic acid (**80**; 71.8 mg, 0.28 mmol), 1-(3-dimethylaminopropyl)-3-ethylcarbodiimide hydrochloride (63.5 mg, 0.33 mmol), 1-hydroxy-1H-benzotriazol-1-ol hydrate (50.7 mg, 0.33 mmol), and *N,N*-diisopropylamine (0.2 mL, 1.1 mmol) in DMF (10 mL) at 0 °C under an atmosphere of nitrogen was added the commercially available 4-(3,4-dimethoxyphenyl)thiophen-2-amine hydrochloride (75 mg, 0.28 mmol) after 1 h. The reaction mixture was allowed to warm to ambient temperature and stirred for 72 h. The product mixture was diluted with EtOAc (20 mL), extracted from water (3 × 10 mL), dried, and concentrated. Purification by preparative HPLC at low pH followed by trituration with Et₂O furnished **80** (yellow solid, 120 mg, 91%). ¹H NMR (CDCl₃): δ 10.30 (s, 1H), 8.02 (s, 1H), 7.56–7.62 (m, 2H), 7.35–7.46 (m, 3H), 7.05–7.12 (m, 2H), 6.89–6.98 (m, 2H), 6.68 (d, *J* = 1.7 Hz, 1H), 5.53 (s, 2H), 3.97 (s, 3H), 3.94 (s, 3H), 3.61 (s, 3H).

[4-(3,4-Dimethoxyphenyl)-2-thienyl]-(3-dimethoxyphosphoryl-carbonyl)-1-piperidylmethanone, 85. Compound **85** was prepared according to the literature²⁹ to furnish the product as a beige gum (83 mg, 16% yield). ¹H NMR (DMSO-*d*₆): δ 6.94–8.87 (m, 5H- mixture of rotomers), 3.55–5.15 (m, 12H- mixture of rotomers), 2.98–3.44

(m, 2H- mixture of rotomers), 2.47–2.53 (m, 3H- mixture of rotomers), 2.21–2.41 (m, 1H- mixture of rotomers), 1.86–2.08 (m, 1H- mixture of rotomers), 1.21–1.78 (m, 2H- mixture of rotomers).

3-[4-(3,4-Dimethoxyphenyl)-2-thienyl]-N-methylsulfonyl-benzamide, 93.³⁷ A suspension of methanesulfonamide (61.5 mg, 0.65 mmol), 3-[4-(3,4-dimethoxyphenyl)-2-thienyl]benzoic acid (**91**; 200 mg, 0.59 mmol), 1-(3-dimethylaminopropyl)-3-ethylcarbodiimide hydrochloride (135.2 mg, 0.71 mmol), and 4-dimethylaminopyridine (35.9 mg, 0.29 mmol) in THF (3 mL) was stirred at ambient temperature for 16 h. The reaction mixture was diluted with water (10 mL) and washed with EtOAc (3 mL). The aqueous layer was acidified to pH 1 with 2 N HCl (aq) (5 mL) and extracted into EtOAc (3 × 10 mL). The combined organic layers were washed with brine (5 mL), dried, and concentrated. The crude product was purified by preparative HPLC at high pH to afford **93** (white solid, 5.2 mg, 2%). ¹H NMR (DMSO-*d*₆): δ 8.16–8.24 (m, 1H), 7.72–8.00 (m, 4H), 7.30–7.46 (m, 3H), 7.00 (d, *J* = 8.3 Hz, 1H), 3.79 (s, 3H), 2.46–2.54 (m, 6H).

4-[4-(3,4-Dimethoxyphenyl)-2-thienyl]-N-methylsulfonyl-benzamide, 94.³⁷ A suspension of methanesulfonamide (27.7 mg, 0.29 mmol), acid **92** (90 mg, 0.26 mmol), 1-(3-dimethylaminopropyl)-3-ethylcarbodiimide hydrochloride (60.8 mg, 0.32 mmol), and 4-dimethylaminopyridine (16.2 mg, 0.13 mmol) in THF (3 mL) was stirred at ambient temperature for 16 h. The reaction mixture was diluted with water (10 mL) and washed with EtOAc (3 mL). The aqueous layer was acidified to pH 1 with 2 N HCl (aq) (5 mL) and extracted into EtOAc (3 × 10 mL). The combined organic layers were washed with brine (5 mL), dried, and concentrated. The crude product was purified by preparative HPLC at high pH to give **94** (white solid, 2.1 mg, 2%). ¹H NMR (DMSO-*d*₆): δ 8.33 (s, 1H), 8.02–8.08 (m, 1H), 7.98 (d, *J* = 8.1 Hz, 2H), 7.78–7.82 (m, 1H), 7.71 (d, *J* = 8.0 Hz, 2H), 7.31–7.41 (m, 2H), 7.00 (d, *J* = 8.6 Hz, 1H), 3.80 (s, 3H), 2.42–2.56 (m, 6H).

N-[4-(3,4-Dimethoxyphenyl)-2-thienyl]-3,5-dimethyl-isoxazole-4-carboxamide, 96. 3,5-Dimethyl-4-isoxazolecarboxylic acid (90.9 mg, 0.64 mmol) was heated to reflux in thionyl chloride (2.1 mL, 28.79 mmol) for 5 h. The reaction mixture was evaporated to dryness, redissolved in THF (3 mL), and added to a cooled (0 °C), stirred solution of *N,N*-diisopropylamine (0.13 mL, 0.77 mmol), 4-dimethylaminopyridine (1.36 mg, 0.01 mmol), and 4-(3,4-dimethoxyphenyl)thiophen-2-amine hydrochloride **95** (70 mg, 0.26 mmol) in THF (3 mL). The reaction mixture was stirred at ambient temperature for 1 h before being partitioned between EtOAc (30 mL) and water (30 mL). The organic layer was washed with 5% Na₂CO₃ (aq) (2 × 30 mL) and saturated brine (30 mL), dried, and concentrated. The crude product was purified by preparative HPLC at high pH to give **96** (cream solid, 23.1 mg, 25%). ¹H NMR (DMSO-*d*₆): δ 7.27–7.30 (m, 1H), 7.13–7.22 (m, 3H), 6.98 (d, *J* = 8.4 Hz, 1H), 3.83 (s, 3H), 3.78 (s, 3H), 2.59 (s, 3H), 2.37 (s, 3H).

N-[4-(3,4-Dimethoxyphenyl)-2-thienyl]benzamide, 97. Compound **97** was prepared in a manner analogous to that for **96** (orange solid, 52.4 mg, 47%). ¹H NMR (DMSO-*d*₆): δ 7.98–8.07 (m, 1H), 7.52–7.67 (m, 3H), 7.12–7.30 (m, 4H), 7.00 (d, *J* = 8.6 Hz, 1H), 3.84 (s, 3H), 3.78 (s, 3H).

N-[4-(3,4-Dimethoxyphenyl)-2-thienyl]-1H-imidazole-2-carboxamide, 98. Compound **98** was prepared in a manner analogous to that for **96** (cream solid, 3.2 mg, 4%). ¹H NMR (DMSO-*d*₆): δ 7.42 (br. s, 1H), 7.08–7.26 (m, 3H), 7.00 (d, *J* = 8.5 Hz, 1H), 3.83 (s, 3H), 3.78 (s, 3H).

N-[4-(3,4-Dimethoxyphenyl)-2-thienyl]-1-methyl-imidazole-2-carboxamide, 99. Compound **99** was prepared in a manner analogous to that for **96** (cream solid, 8.6 mg, 10%). ¹H NMR (DMSO-*d*₆): δ 7.47–7.49 (m, 1H), 7.37–7.41 (m, 1H), 7.23–7.26 (m, 1H), 7.17–7.20 (m, 1H), 7.23–7.26 (m, 1H), 7.08–7.14 (m, 2H), 6.99 (d, *J* = 8.1 Hz, 1H), 4.02 (s, 3H), 3.83 (s, 3H), 3.78 (s, 3H).

N-[4-(3,4-Dimethoxyphenyl)-2-thienyl]-3-methyl-isoxazole-5-carboxamide, 100. Compound **100** was prepared in a manner analogous to that for **96** (cream solid, 26.9 mg, 30%). ¹H NMR (DMSO-*d*₆): δ 7.28–7.35 (m, 2H), 7.19–7.22 (m, 1H), 7.10–7.17 (m, 2H), 6.99 (d, *J* = 7.8 Hz, 1H), 3.84 (s, 3H), 3.78 (s, 3H), 2.35 (s, 3H).

N-[4-(3,4-Dimethoxyphenyl)-2-thienyl]-1-methyl-pyrazole-3-carboxamide, 101. Compound **101** was prepared in a manner analogous to that for **96** (white solid, 18.2 mg, 21%). ¹H NMR (DMSO-*d*₆): δ 7.87 (d, *J* = 2.7 Hz, 1H), 7.36 (d, *J* = 1.8 Hz, 1H), 7.17–7.22 (m, 2H), 7.07–7.14 (m, 1H), 6.98 (d, *J* = 8.2 Hz, 1H), 6.79 (d, *J* = 2.2 Hz, 1H), 3.99 (s, 3H), 3.83 (s, 3H), 3.78 (s, 3H).

N-[4-(3,4-Dimethoxyphenyl)-2-thienyl]-4-methyl-thiadiazole-5-carboxamide, 102. Compound **102** was prepared in a manner analogous to that for **96** (cream solid, 6.3 mg, 7%). ¹H NMR (DMSO-*d*₆): δ 7.31–7.35 (m, 1H), 7.13–7.24 (m, 3H), 6.99 (d, *J* = 7.9 Hz, 1H), 3.83 (s, 3H), 3.78 (s, 3H), 2.87 (s, 3H).

N-[4-(3,4-Dimethoxyphenyl)-2-thienyl]-2,4-dimethyl-6-oxopyran-3-carboxamide, 103. *N,N*-Diisopropylamine (0.24 mL, 1.47 mmol) was added to a suspension of the commercially available 4-(3,4-dimethoxyphenyl)thiophen-2-amine hydrochloride **95** (100 mg, 0.37 mmol) in DMF (5 mL). After being stirred at ambient temperature for 15 min, the solution was cooled to 0 °C, and 4,6-dimethyl-2-oxo-2H-pyran-5-carboxylic acid (61.9 mg, 0.37 mmol) and 1-(3-dimethylaminopropyl)-3-ethylcarbodiimide hydrochloride (84.7 mg, 0.44 mmol) were added. The solution was allowed to warm to ambient and left to stir for 16 h. The reaction mixture was concentrated to dryness, partitioned between EtOAc (20 mL) and water (10 mL), and separated. The organic layer was washed with 5% Na₂CO₃ (aq) (2 × 30 mL) and saturated brine (30 mL), dried, and concentrated. The crude product was filtered and washed with Et₂O to afford **103** (pale yellow solid, 22.7 mg, 16%). ¹H NMR (DMSO-*d*₆): δ 13.11 (br. s, 1H), 7.76–7.82 (m, 1H), 7.55–7.63 (m, 1H), 7.21–7.35 (m, 2H), 6.99 (d, *J* = 8.2 Hz, 1H), 5.68 (s, 1H), 3.84 (s, 3H), 3.78 (s, 3H), 2.61 (s, 3H), 2.41 (s, 3H).

1-[4-(3,4-Dimethoxyphenyl)-2-thienyl]-3-phenyl-urea, 104. Compound **104** was prepared according to the literature⁴⁹ by reaction of **95** with phenyl isocyanate to furnish the product as a white solid (22.6 mg, 17% yield). ¹H NMR (DMSO-*d*₆): δ 9.63 (s, 1H), 8.82 (s, 1H), 7.47 (d, *J* = 7.9 Hz, 2H), 7.30 (t, *J* = 7.9 Hz, 2H), 7.10–7.22 (m, 3H), 6.89–7.04 (m, 3H), 3.83 (s, 3H), 3.78 (s, 3H).

10-Methylpyrimido[4,5-*b*]quinoline-2,4-dione, 130.³³ Prepared according to the literature (yellow solid, 6.5 mg, 8%). ¹H NMR (DMSO-*d*₆): δ 9.00 (s, 1H), 8.19 (d, *J* = 8.0 Hz, 1H), 7.92–8.00 (m, 2H), 7.55 (dd, *J* = 7.0, 2.0 Hz, 1H), 4.04 (s, 3H).

9-Chloro-10-phenyl-pyrimido[4,5-*b*]quinoline-2,4-dione, 134. A suspension of 3-chloro-2-fluorobenzaldehyde (65.6 mg, 0.41 mmol) and 6-anilino-1H-pyrimidine-2,4-dione (**106**; 70.0 mg, 0.34 mmol) in DMF (2 mL) was heated by microwave irradiation at 110 °C for 30 min. Water (20 mL) was added to the reaction mixture, and the resulting precipitate was filtered and washed with water. The filtered solid was dried under vacuum and then purified by preparative HPLC at high pH to yield the product **134** as a yellow solid (20.4 mg, 18%). ¹H NMR (DMSO-*d*₆): δ 11.6 (s, 1H), 9.10 (s, 1H), 8.25 (dd, *J* = 8.0, 1.6 Hz, 1H), 7.84 (dd, *J* = 8.0, 1.6 Hz, 1H), 7.38–7.53 (m, 6H).

7-Chloro-10-phenyl-pyrimido[4,5-*b*]quinoline-2,4-dione, 135. Compound **135** was prepared in a manner analogous to that for **134** (yellow solid, 1.56 mg, 2%). ¹H NMR (DMSO-*d*₆): δ 9.10 (s, 1H), 8.39 (d, *J* = 2.5 Hz, 1H), 7.64–7.78 (m, 4H), 7.42–7.45 (m, 2H), 6.71 (d, *J* = 9.3 Hz, 1H).

6-Chloro-10-phenyl-pyrimido[4,5-*b*]quinoline-2,4-dione, 136.³⁴ Compound **136** was prepared in a manner analogous to that for **134** (yellow solid, 63.5 mg, 57%). ¹H NMR (DMSO-*d*₆): δ 11.2 (s, 1H), 9.03 (d, *J* = 0.7 Hz, 1H), 7.64–7.74 (m, 5H), 7.42–7.45 (m, 2H), 6.69 (ddd, *J* = 7.3, 2.4, 0.9 Hz, 1H). LC-MS *m/z* 324.5, 326.5 [M + H]⁺, 89% purity.

8-Chloro-10-methyl-pyrimido[4,5-*b*]quinoline-2,4-dione, 137. Compound **137** was prepared in a manner analogous to that for **134** (yellow solid, 86.9 mg, 67%). ¹H NMR (DMSO-*d*₆): δ 11.1 (s, 1H), 9.00 (s, 1H), 8.21 (d, *J* = 8.6 Hz, 1H), 8.04 (d, *J* = 1.7 Hz, 1H), 7.61 (dd, *J* = 8.6, 1.7 Hz, 1H), 4.01 (s, 3H).

8-Chloro-10-cyclopropyl-pyrimido[4,5-*b*]quinoline-2,4-dione, 138. Compound **138** was prepared in a manner analogous to that for **134** (yellow solid, 80.4 mg, 67%). ¹H NMR (DMSO-*d*₆): δ 11.1 (s, 1H), 8.92 (s, 1H), 8.15–8.18 (m, 2H), 7.57 (dd, *J* = 8.5, 1.8 Hz, 1H), 1.42–1.49 (m, 2H), 1.23 (s, 1H), 0.92–0.97 (m, 2H).

8-Chloro-10-cyclohexyl-pyrimido[4,5-*b*]quinoline-2,4-dione, 139. Compound **139** was prepared in a manner analogous to that for **134** (yellow solid, 13.4 mg, 12%). ¹H NMR (DMSO-*d*₆): δ 11.2 (s, 1H), 8.96 (s, 1H), 8.20 (d, *J* = 8.5 Hz, 1H), 7.59 (d, *J* = 8.5 Hz, 1H), 1.06–1.89 (m, 11H).

8-Chloro-10-(4-piperidyl)pyrimido[4,5-*b*]quinoline-2,4-dione, 140. Compound **140** was prepared in a manner analogous to that for **134**, with an additional deprotection step of the N-Boc piperidyl precursor with DCM/TFA (3:1 v/v) at ambient temperature (yellow solid, 37.2 mg, 23%). ¹H NMR (DMSO-*d*₆): δ 8.97 (s, 1H), 8.38 (s, 2H), 8.32 (br. s, 1H), 8.21 (d, *J* = 8.6 Hz, 1H), 7.60 (dd, *J* = 8.6, 1.1 Hz, 1H), 3.30 (app. d, *J* = 9.5 Hz, 2H), 2.61–3.10 (m, 4H), 1.81 (app. d, *J* = 9.5 Hz, 2H).

8-Chloro-10-(4-hydroxyphenyl)pyrimido[4,5-*b*]quinoline-2,4-dione, 141. Compound **141** was prepared in a manner analogous to that for **134** (yellow solid, 81.1 mg, 75%). ¹H NMR (DMSO-*d*₆): δ 11.1 (s, 1H), 10.0 (s, 1H), 9.10 (s, 1H), 8.26 (d, *J* = 8.6 Hz, 1H), 7.57 (dd, *J* = 8.6, 1.9 Hz, 1H), 7.20 (app. d, *J* = 8.6 Hz, 2H), 7.02 (app. d, *J* = 8.6 Hz, 2H), 6.70 (d, *J* = 1.9 Hz, 1H). ¹³C NMR (DMSO-*d*₆): δ 161.8, 159.1, 158.1, 156.4, 143.1, 141.5, 139.3, 133.1, 129.3, 128.1, 124.6, 119.8, 116.7, 116.4, 115.9. HRMS (ESI) *m/z* [M + H]⁺ calcd for C₁₇H₁₁N₃O₃Cl: 340.0484. Found: 340.0482.

8-Chloro-10-(4-methoxyphenyl)pyrimido[4,5-*b*]quinoline-2,4-dione, 142. Compound **142** was prepared in a manner analogous to that for **134** (yellow solid, 82.9 mg, 78%). ¹H NMR (DMSO-*d*₆): δ 11.1 (s, 1H), 9.12 (s, 1H), 8.27 (d, *J* = 8.6 Hz, 1H), 7.58 (dd, *J* = 8.6 Hz, 1H), 7.36 (app. d, *J* = 8.9 Hz, 2H), 7.23 (app. d, *J* = 8.9 Hz, 2H), 6.68 (d, *J* = 1.9 Hz, 1H), 3.89 (s, 3H).

8-Chloro-10-(3-hydroxyphenyl)pyrimido[4,5-*b*]quinoline-2,4-dione, 143. Compound **143** was prepared in a manner analogous to that for **134** (yellow solid, 25.9 mg, 33%). ¹H NMR (DMSO-*d*₆): δ 11.1 (br. s, 1H), 10.1 (br. s, 1H), 9.11 (s, 1H), 8.26 (d, *J* = 8.8 Hz, 1H), 7.58 (dd, *J* = 8.5, 1.8 Hz, 1H), 7.48 (t, *J* = 8.0 Hz, 1H), 7.03 (app. dd, *J* = 8.3, 2.3 Hz, 1H), 6.79–6.84 (m, 2H), 6.68 (d, *J* = 1.8 Hz, 1H). ¹³C NMR (DMSO-*d*₆): δ 161.7, 158.9, 158.6, 156.4, 142.4, 141.6, 139.2, 138.0, 133.1, 131.1, 124.7, 119.8, 118.4, 116.6, 116.3, 115.9, 115.1. HRMS (ESI) *m/z* [M + H]⁺ calcd for C₁₇H₁₁N₃O₃Cl: 340.0484. Found: 340.0482.

8-Chloro-10-(2-hydroxyphenyl)pyrimido[4,5-*b*]quinoline-2,4-dione, 144. Compound **144** was prepared in a manner analogous to that for **134** (yellow solid, 85.7 mg, 79%). ¹H NMR (DMSO-*d*₆): δ 11.2 (s, 1H), 10.0 (s, 1H), 9.1 (s, 1H), 8.27 (d, *J* = 8.6 Hz, 1H), 7.59 (dd, *J* = 8.5, 1.8 Hz, 1H), 7.47 (app. t, *J* = 7.8 Hz, 1H), 7.29 (dd, *J* = 7.8, 1.5 Hz, 1H), 7.15 (d, *J* = 8.5 Hz, 1H), 7.08 (t, *J* = 7.8 Hz, 1H), 6.68 (d, *J* = 1.8 Hz, 1H).

10-Phenyl-8-(trifluoromethyl)pyrimido[4,5-*b*]quinoline-2,4-dione, 145. Compound **145** was prepared in a manner analogous to that for **134** (yellow solid, 21.7 mg, 25%). ¹H NMR (DMSO-*d*₆): δ 11.2 (br. s, 1H), 9.21 (s, 1H), 8.48 (d, *J* = 7.9 Hz, 1H), 7.84 (dd, *J* = 8.4, 1.4 Hz, 1H), 7.64–7.76 (m, 3H), 7.47–7.50 (m, 2H), 6.82 (s, 1H). ¹³C NMR (DMSO-*d*₆): δ 161.5, 159.0, 156.3, 141.5, 141.3, 137.0, 133.0, 130.4, 129.8, 128.3, 123.3, 120.1, 118.0, 117.7, 113.4 (CF₃ not observed). HRMS (ESI) *m/z* [M + H]⁺ calcd for C₁₈H₁₁N₃O₂F₃: 358.0798. Found: 358.0798.

2,4-Dioxo-10-phenyl-pyrimido[4,5-*b*]quinoline-8-carbonitrile, 146. Compound **146** was prepared in a manner analogous to that for **134** (yellow solid, 52.7 mg, 68%). ¹H NMR (DMSO-*d*₆): δ 11.3 (s, 1H), 9.17 (s, 1H), 8.42 (d, *J* = 8.1 Hz, 1H), 7.89 (dd, *J* = 8.1, 1.4 Hz, 1H), 7.64–7.76 (m, 3H), 7.43–7.47 (m, 2H), 7.01 (s, 1H). ¹³C NMR (DMSO-*d*₆): δ 161.4, 158.9, 156.2, 141.3, 141.1, 136.8, 132.5, 130.4, 129.7, 128.4, 126.3, 123.6, 120.8, 118.2, 117.7, 115.6. HRMS (ESI) *m/z* [M + H]⁺ calcd for C₁₈H₁₁N₃O₂: 315.0877. Found: 315.0882.

10-(3-Hydroxyphenyl)-2,4-dioxo-pyrimido[4,5-*b*]quinoline-8-carbonitrile, 147. Compound **147** was prepared in a manner analogous to that for **134** (yellow solid, 31.7 mg, 42%). ¹H NMR (DMSO-*d*₆): δ 11.2 (br. s, 1H), 10.1 (br. s, 1H), 9.14 (s, 1H), 8.40 (d, *J* = 8.1 Hz, 1H), 7.88 (dd, *J* = 8.1, 1.4 Hz, 1H), 7.49 (t, *J* = 8.1 Hz, 1H), 7.09 (s, 1H), 7.04 (app. d, *J* = 8.1 Hz, 1H), 6.79–6.83 (m, 2H). ¹³C NMR (DMSO-*d*₆): δ 161.5, 158.9, 158.7, 156.3, 141.2, 141.0, 137.7, 132.4, 131.1, 126.2, 123.6, 120.9, 118.4, 118.2, 117.7, 116.7, 115.6, 115.2.

HRMS (ESI) *m/z* [M + H]⁺ calcd for C₁₈H₁₁N₄O₃: 331.0826. Found: 331.0820.

10-(4-Hydroxyphenyl)-2,4-dioxo-pyrimido[4,5-*b*]quinoline-8-carbonitrile, 148. Compound **148** was prepared in a manner analogous to that for **134** (orange solid, 49.8 mg, 47%). ¹H NMR (DMSO-*d*₆): δ 11.2 (br. s, 1H), 10.1 (br. s, 1H), 9.14 (s, 1H), 8.39 (d, *J* = 8.1 Hz, 1H), 7.87 (dd, *J* = 8.1, 1.4 Hz, 1H), 7.19 (app. d, *J* = 8.8 Hz, 2H), 7.12 (s, 1H), 7.03 (app. d, *J* = 8.8 Hz, 2H). ¹³C NMR (DMSO-*d*₆): δ 161.5, 159.2, 158.3, 156.3, 141.9, 140.9, 132.4, 129.3, 127.7, 126.2, 123.6, 121.1, 118.2, 117.7, 116.7, 115.6. HRMS (ESI) *m/z* [M + H]⁺ calcd for C₁₈H₁₁N₄O₃: 331.0826. Found: 331.0819.

10-[3-(Hydroxymethyl)phenyl]-2,4-dioxo-pyrimido[4,5-*b*]quinoline-8-carbonitrile, 149. Compound **149** was prepared in a manner analogous to that for **134** (yellow solid, 11 mg, 11%). ¹H NMR (DMSO-*d*₆): δ 11.20 (s, 1H), 9.17 (s, 1H), 8.42 (d, *J* = 8.6 Hz, 1H), 7.90 (dd, *J* = 8.2, 1.4 Hz, 1H), 7.67 (t, *J* = 8.0 Hz, 1H), 7.60 (app. d, *J* = 8.0 Hz, 1H), 7.37 (br. s, 1H), 7.28–7.32 (m, 1H), 7.00 (s, 1H), 5.42 (t, *J* = 5.8 Hz, 1H), 4.64 (d, *J* = 5.8 Hz, 2H). ¹³C NMR (DMSO-*d*₆): δ 161.5, 158.9, 156.3, 145.4, 141.3, 141.0, 136.7, 132.5, 130.1, 127.4, 126.5, 126.3, 125.8, 123.6, 120.8, 118.2, 115.6, 66.3. HRMS (ESI) *m/z* [M + H]⁺ calcd for C₁₉H₁₃N₄O₃: 345.0983. Found: 345.0984.

10-(3-Methoxyphenyl)-2,4-dioxo-pyrimido[4,5-*b*]quinoline-8-carbonitrile, 150. Compound **150** was prepared in a manner analogous to that for **134** (yellow solid, 10 mg, 14%). ¹H NMR (DMSO-*d*₆): δ 11.26 (s, 1H), 9.16 (s, 1H), 8.40 (d, *J* = 8.6 Hz, 1H), 7.88 (dd, *J* = 8.6, 1.3 Hz, 1H), 7.62 (t, *J* = 8.6 Hz, 1H), 7.23 (ddd, *J* = 8.4, 2.6, 0.8 Hz, 1H), 7.09 (app. t, *J* = 0.8 Hz, 1H), 7.06 (dd, *J* = 2.4, 1.8 Hz, 1H), 6.99 (ddd, *J* = 8.4, 2.6, 0.8 Hz, 1H), 3.82 (s, 3H). LC-MS *m/z* 343.5, [M – H][–], 91% purity.

10-(4-Methoxyphenyl)-2,4-dioxo-pyrimido[4,5-*b*]quinoline-8-carbonitrile, 151. Compound **151** was prepared in a manner analogous to that for **134** (yellow solid, 88.6 mg, 86%). ¹H NMR (DMSO-*d*₆): δ 11.2 (s, 1H), 9.15 (s, 1H), 8.40 (d, *J* = 8.1 Hz, 1H), 7.88 (dd, *J* = 8.1, 1.4 Hz, 1H), 7.35 (app. d, *J* = 8.9 Hz, 2H), 7.23 (app. d, *J* = 8.9 Hz, 2H), 7.12 (s, 1H), 3.90 (s, 3H). ¹³C NMR (DMSO-*d*₆): δ 161.5, 159.7, 159.2, 156.3, 141.7, 141.0, 132.4, 129.4, 129.2, 126.2, 123.6, 121.0, 118.2, 117.7, 115.5, 55.5. HRMS (ESI) *m/z* [M + H]⁺ calcd for C₁₉H₁₃N₄O₃: 345.0983. Found: 345.0989.

10-(3-Hydroxy-4-methoxy-phenyl)-2,4-dioxo-pyrimido[4,5-*b*]quinoline-8-carbonitrile, 152. Compound **152** was prepared in a manner analogous to that for **134** (orange solid, 12.0 mg, 8%). ¹H NMR (DMSO-*d*₆): δ 11.22 (br. s, 1H), 9.58 (br. s, 1H), 9.13 (s, 1H), 8.38 (d, *J* = 8.6 Hz, 1H), 7.87 (dd, *J* = 8.6, 1.3 Hz, 1H), 7.16–7.20 (m, 2H), 6.77–6.81 (m, 2H), 3.90 (s, 3H).

10-(3-Fluorophenyl)-2,4-dioxo-pyrimido[4,5-*b*]quinoline-8-carbonitrile, 153. Compound **153** was prepared in a manner analogous to that for **134** (yellow solid, 22.0 mg, 14%). ¹H NMR (DMSO-*d*₆): δ 11.29 (s, 1H), 9.18 (s, 1H), 8.41 (d, *J* = 8.6 Hz, 1H), 7.90 (dd, *J* = 8.6, 1.3 Hz, 1H), 7.77 (td, *J* = 8.1, 6.4 Hz, 1H), 7.53 (tdd, *J* = 8.6, 1.9, 0.8 Hz, 1H), 7.43 (ddd, *J* = 9.4, 2.7, 1.5 Hz, 1H), 7.38 (ddd, *J* = 8.0, 1.4, 0.8 Hz, 1H), 7.22 (s, 1H).

10-(4-Bromophenyl)-2,4-dioxo-pyrimido[4,5-*b*]quinoline-8-carbonitrile, 154. Compound **154** was prepared in a manner analogous to that for **134** (yellow solid, 22.6 mg, 23%). ¹H NMR (DMSO-*d*₆): δ 9.17 (s, 1H), 8.41 (d, *J* = 8.1 Hz, 1H), 7.88–7.92 (m, 3H), 7.42 (app. d, *J* = 8.6 Hz, 2H), 7.26 (s, 1H). ¹³C NMR (DMSO-*d*₆): δ 161.4, 159.0, 156.1, 141.2, 141.1, 136.1, 133.5, 130.7, 126.5, 124.2, 123.6, 123.0, 121.1, 117.7, 115.9. LC-MS *m/z* 393.4 [M + H]⁺, 92% purity. HRMS (ESI) *m/z* [M + H]⁺ calcd for C₁₈H₁₀N₄O₂Br: 392.9982. Found: 392.9979.

10-(3-Aminophenyl)-2,4-dioxo-pyrimido[4,5-*b*]quinoline-8-carbonitrile, 155. Compound **155** was prepared in a manner analogous to that for **134**, with an additional deprotection step of the N-Boc aminophenyl precursor with DCM/TFA (3:1 v/v) (11.5 mL) at ambient temperature for 2 h (orange solid, 17.2 mg, 17%). ¹H NMR (DMSO-*d*₆): δ 11.2 (br. s, 1H), 9.13 (s, 1H), 8.39 (d, *J* = 8.1 Hz, 1H), 7.87 (dd, *J* = 8.1, 1.4 Hz, 1H), 7.31 (t, *J* = 7.8 Hz, 1H), 7.01 (s, 1H), 6.80 (app. d, *J* = 8.1 Hz, 1H), 6.45–6.50 (m, 2H), 5.56 (br. s, 2H). ¹³C NMR (DMSO-*d*₆): δ 161.5, 158.5, 156.3, 150.7, 141.2, 140.9, 137.5, 132.3, 130.7, 126.1, 123.5, 121.0, 118.2, 115.5, 114.8, 114.4, 112.6.

HRMS (ESI) m/z $[M + H]^+$ calcd for $C_{18}H_{12}N_5O_2$: 330.0986. Found: 330.0979.

N-[3-(8-Cyano-2,4-dioxo-pyrimido[4,5-*b*]quinolin-10-yl)phenyl]-acetamide, **156**. Compound **156** was prepared in a manner analogous to that for **134** (yellow solid, 12.0 mg, 17%). 1H NMR (DMSO- d_6): δ 11.24 (s, 1H), 10.31 (s, 1H), 9.15 (s, 1H), 8.41 (d, $J = 8.1$ Hz, 1H), 7.90 (dd, $J = 8.1, 1.4$ Hz, 1H), 7.78–7.80 (m, 1H), 7.67–7.72 (m, 1H), 7.65 (t, $J = 8.0$ Hz, 1H), 7.06–7.10 (m, 2H) 3.03 (s, 3H). HRMS (ESI) m/z $[M + H]^+$ calcd for $C_{20}H_{14}N_5O_3$: 372.1092. Found: 372.1097.

N-[3-(8-Cyano-2,4-dioxo-pyrimido[4,5-*b*]quinolin-10-yl)phenyl]-methanesulfonamide, **157**. Compound **157** was prepared in a manner analogous to that for **134** (yellow solid, 28.0 mg, 20%). 1H NMR (DMSO- d_6): δ 11.16 (s, 1H), 10.15 (s, 1H), 9.14 (s, 1H), 8.40 (d, $J = 8.6$ Hz, 1H), 7.89 (dd, $J = 8.2, 1.4$ Hz, 1H), 7.66 (t, $J = 8.0$ Hz, 1H), 7.43 (ddd, $J = 8.2, 2.4, 1.0$ Hz, 1H), 7.23 (dd, $J = 2.4, 1.4$ Hz, 1H), 7.20 (app. t, $J = 0.6$ Hz, 1H), 7.14 (ddd, $J = 8.2, 2.4, 1.0$ Hz, 1H), 3.11 (s, 3H).

N-[3-(2,4-Dioxopyrimido[4,5-*b*]quinolin-10-yl)phenyl]-methanesulfonamide, **158**. Compound **158** was prepared in a manner analogous to that for **134** (yellow solid, 5.0 mg, 4%). 1H NMR (DMSO- d_6): δ 11.09 (s, 1H), 10.26 (br. s, 1H), 9.12 (s, 1H), 8.24 (d, $J = 8.0$ Hz, 1H), 7.76 (t, $J = 8.0$ Hz, 1H), 7.64 (t, $J = 8.0$ Hz, 1H), 7.52 (t, $J = 8.0$ Hz, 1H), 7.42 (d, $J = 8.2$ Hz, 1H), 7.19 (s, 1H), 7.13 (d, $J = 8.2$ Hz, 1H), 6.81 (d, $J = 8.2$ Hz, 1H), 3.09 (s, 3H).

N-[3-(7-Chloro-2,4-dioxo-pyrimido[4,5-*b*]quinolin-10-yl)phenyl]-methanesulfonamide, **159**. Compound **159** was prepared in a manner analogous to that for **134** (yellow solid, 12.0 mg, 28%). 1H NMR (DMSO- d_6): δ 10.94 (s, 1H), 9.99 (s, 1H), 8.86 (s, 1H), 8.16 (d, $J = 2.4$ Hz, 1H), 7.54 (dd, $J = 9.2, 1.1$ Hz, 1H), 7.44 (t, $J = 8.0$ Hz, 1H), 7.21 (app. d, $J = 8.2$ Hz, 1H), 6.99 (t, $J = 2.0$ Hz, 1H), 6.92 (app. d, $J = 8.2$ Hz, 1H), 6.60 (d, $J = 9.2$ Hz, 1H), 2.89 (s, 3H). LC-MS m/z 417.5 $[M + H]^+$, 94% purity. HRMS (ESI) m/z $[M + Na]^+$ calculated for $C_{18}H_{13}N_4O_4NaCl$: 439.0239. Found: 439.0231.

3-(8-Cyano-2,4-dioxo-pyrimido[4,5-*b*]quinolin-10-yl)-benzenesulfonamide, **160**. Compound **160** was prepared in a manner analogous to that for **134** (yellow solid, 8.0 mg, 6%). 1H NMR (DMSO- d_6): δ 11.28 (br. s, 1H), 9.17 (s, 1H), 8.43 (d, $J = 8.6$ Hz, 1H), 8.12 (app. d, $J = 8.0$ Hz, 1H), 7.89–7.97 (m, 3H), 7.71 (app. d, $J = 8.0$ Hz, 1H), 7.61 (br. s, 2H), 7.05 (s, 1H).

10-(1*H*-Indazol-6-yl)-2,4-dioxo-pyrimido[4,5-*b*]quinoline-8-carbonitrile, **161**. Compound **161** was prepared in a manner analogous to that for **134** (orange solid, 26.2 mg, 26%). 1H NMR (DMSO- d_6): δ 13.46 (s, 1H), 11.18 (br. s, 1H), 9.10 (s, 1H), 8.42 (d, $J = 8.6$ Hz, 1H), 8.29 (s, 1H), 8.06 (dd, $J = 8.6, 0.4$ Hz, 1H), 7.88 (dd, $J = 8.2, 1.4$ Hz, 1H), 7.69 (s, 1H), 7.17 (s, 1H), 7.10 (dd, $J = 8.6, 0.4$ Hz, 1H). ^{13}C NMR (DMSO- d_6): δ 161.5, 159.2, 156.3, 141.6, 141.1, 140.2, 134.6, 133.9, 132.3, 126.3, 123.5, 123.2, 122.6, 121.2, 120.2, 118.2, 115.7, 110.6. HRMS (ESI) m/z $[M + H]^+$ calcd for $C_{19}H_{11}N_6O_2$: 355.0938. Found: 355.0942.

10-(1*H*-Indazol-4-yl)-2,4-dioxo-pyrimido[4,5-*b*]quinoline-8-carbonitrile, **162**. Compound **162** was prepared in a manner analogous to that for **134** (yellow solid, 4.0 mg, 4%). 1H NMR (DMSO- d_6): δ 13.53 (s, 1H), 11.18 (s, 1H), 9.23 (s, 1H), 8.42 (d, $J = 8.6$ Hz, 1H), 7.82–7.90 (m, 3H), 7.64 (t, $J = 8.0, 1H$), 7.21 (d, $J = 7.3$ Hz, 1H), 6.99 (s, 1H).

2,4-Dioxo-10-[3-(1*H*-tetrazol-5-yl)phenyl]pyrimido[4,5-*b*]quinoline-8-carbonitrile, **163**. Compound **163** was prepared in a manner analogous to that for **134** (yellow solid, 15.1 mg, 11%). 1H NMR (DMSO- d_6): δ 11.28 (s, 1H), 9.19 (s, 1H), 8.43 (d, $J = 8.6$ Hz, 1H), 8.27 (ddd, $J = 8.0, 1.6, 1.0$ Hz, 1H), 8.14 (s, 1H), 7.91 (dd, $J = 8.2, 1.4$ Hz, 1H), 7.87–7.92 (m, 2H), 7.59 (ddd, $J = 8.0, 2.0, 1.0$ Hz, 1H), 7.23 (s, 1H).

Biological Assay Protocols. TDP2 Chromogenic Assay. The assay was performed in 384-well clear plates in a final volume of 25 μ L comprised of reaction buffer (25 mM Hepes (pH 8.0), 10 mM $MgCl_2$, 130 mM KCl, 1 mM dithiothreitol (DTT)), 0.03% bovine serum albumin (BSA), 1% dimethyl sulfoxide (DMSO) with or without inhibitory compound, and 36 nM TDP2 protein. The reaction was initiated by the addition of 20 mM 4-nitrophenyl phenylphosphonate (NPPP), and the assay was allowed to proceed at 25 °C for 60 min

before being stopped with the addition of 33 mM ethylenediaminetetraacetic acid (EDTA). The signal generated during the assay was quantified by absorbance at 405 nm using a BioTek Synergy 2 multimode microplate reader.

TDP2 Oligonucleotide Assay. A 50-phosphotyrosyl oligonucleotide (50-Y-TCCGTTGAAGCCTGCTTT-30) was purchased from Midland Certified Reagent (USA). Assays were assembled in a final volume of 25 μ L in 384-well clear plates in a buffer composed of 25 mM Hepes (pH 8.0), 10 mM $MgCl_2$, 130 mM KCl, 1 mM DTT, 0.03% BSA, 1% DMSO with or without inhibitory compound, 1.5 U of calf intestinal alkaline phosphatase (CIP, Roche), and 0.36 nM TDP2 protein. The reaction was initiated by the addition of 25 μ L of 1 M 50-phosphotyrosyl oligonucleotide, and the assay was allowed to proceed at 25 °C for 60 min. Then, 25 μ L of Biomol Green reagent (Enzo Life Sciences) was added to stop and develop the reaction. Following further incubation for 45 min, the absorbance was read at 620 nm using a BioTek Synergy 2 multimode microplate reader.

TDP1 Assay. The assay was performed in 384-well black plates in a 25 μ L final volume with a reaction buffer composed of 50 mM Tris HCl, pH 7.5, 2 mM $MgCl_2$, 25 mM NaCl, 1 mM DTT, 0.01% Tween-20, 1% DMSO, 5 nM TDP1, and 50 nM labeled double-stranded AP-site containing DNA substrate. The oligonucleotides 5'-GAG TCG TAC GAG GGT GA-[BHQ2]-3', where BHQ2 is Black Hole Quencher-2, and 5'-[TAM]-TCA CCG TCG TAC GAC TC-3', where TAM is TAMRA and Φ is dSpacer, were annealed together to create the double-stranded DNA substrate. The assay was allowed to proceed at 25 °C for 30 min before stopping with the addition of 0.08% SDS. The fluorescent signal generated during the assay was quantified with excitation at 540 nm and emission at 590 nm using a BioTek Synergy 2 multimode microplate reader.

APE-1 Assay. APE-1 enzyme was obtained from New England Biolabs Inc. The assay was performed in 384-well black plates in a 25 μ L final volume with a reaction buffer composed of 50 mM Tris HCl, pH 7.5, 2 mM $MgCl_2$, 25 mM NaCl, 1 mM DTT, 0.01% Tween-20, 1% DMSO, 50 nM labeled double-stranded AP-site containing DNA substrate, as described above, and 0.03 nM APE1. The assay was allowed to proceed for 30 min at 25 °C before being stopped with the addition of 18 mM EDTA. Fluorescence was measured with excitation at 540 nm and emission at 590 nm.

■ ASSOCIATED CONTENT

📄 Supporting Information

Summary of purity data, LC-MS methods and solvent gradients, preparative HPLC instrument and solvent gradients, preparative methods and spectroscopic data for intermediates **3–23**, **32–68**, **71,72**, **74–76**, **80**, **83–85**, **89–92**, and **106–127**, 1H NMR spectra of target compounds, additional references, dose–response curves of selected toxoflavins and active deazaflavins for the TDP2 chromogenic assay, and method for generating computational docking poses for the deazaflavins. This material is available free of charge via the Internet at <http://pubs.acs.org>.

■ AUTHOR INFORMATION

Corresponding Author

*Telephone: +44 (0)161-918-7447. E-mail: araoof@picr.man.ac.uk.

Notes

The authors declare no competing financial interest.

■ ACKNOWLEDGMENTS

This work was supported by Cancer Research UK (Grant C480/A11411). The TDP2 enzyme was cloned and purified by E. McKenzie at the Protein Expression Facility, Manchester Interdisciplinary Biocentre, U.K. HRMS spectra were generated by R. Sung, School of Chemistry, University of Manchester,

M13 9PL, U.K. *In vitro* DMPK data were provided by Cyprotex Discovery, Macclesfield, U.K. JChem for Excel was used for structure–property prediction and calculation, and general data handling (JChem for Excel, version 5.4.0.411, 2008–2009, ChemAxon, <http://www.chemaxon.com>). We thank James Smith (Cancer Research Technology Ltd.) for triaging HTS output, Andy Barker for providing input and advice for alternative scaffolds to the toxoflavins, and H. Nikki March (Cancer Research UK Drug Discovery Unit, Paterson Institute for Cancer Research) for proofreading the manuscript and helpful comments.

ABBREVIATIONS USED

APE1, apurinic/aprimidinic endonuclease; app, apparent; Caco-2, heterogeneous human epithelial colorectal adenocarcinoma cells; DIPEA, diisopropylethylamine; EDCl, 1-ethyl-3-(3-dimethylaminopropyl)carbodiimide; ES[−], negative ion electrospray ionization; ES⁺, positive ion electrospray ionization; HOBt, hydroxybenzotriazole; HRP, horseradish peroxidase; NPPP, 4-nitrophenyl phenylphosphonate; SQD, single quadrupole detector; TAM, tetramethylrhodamine; TAMRA, tetramethylrhodamine; TDP1, tyrosyl-DNA phosphodiesterase I; TDP2, tyrosyl-DNA phosphodiesterase II; UPLC, ultra performance liquid chromatography; μ W, microwave; EAPII, ETS1-associated protein II; TTRAP, TRAF and TNF receptor-associated protein

REFERENCES

- (1) Thomson, G.; Watson, A.; Caldecott, K.; Denny, O.; Depledge, P.; Hamilton, N.; Hopkins, G.; Jordan, A.; Morrow, C.; Raouf, A.; Waddell, I.; Ogilvie, D. Generation of assays and antibodies to facilitate the study of human 5'-tyrosyl DNA phosphodiesterase. *Anal. Biochem.* **2013**, *436*, 145–150.
- (2) Cortes Ledesma, F.; El Khamisy, S. F.; Zuma, M. C.; Osborn, K.; Caldecott, K. A human 5'-tyrosyl DNA phosphodiesterase that repairs topoisomerase-mediated DNA damage. *Nature* **2009**, *461*, 674–678.
- (3) Moore, J. K.; Haber, J. E. Cell cycle and genetic requirements of two pathways of nonhomologous end-joining repair of double-strand breaks in *Saccharomyces cerevisiae*. *Mol. Cell. Biol.* **1996**, *16*, 2164–2173.
- (4) San Filippo, J.; Sung, P.; Klein, H. Mechanism of eukaryotic homologous recombination. *Annu. Rev. Biochem.* **2008**, *77*, 229–257.
- (5) Bahmad, K.; Nitiss, K. C.; Nitiss, J. L. UnTrapping the ends: A new player in overcoming protein linked DNA damage. *Cell Res.* **2010**, *20*, 122–123.
- (6) Wei, H.; Ruthenburg, A. J.; Bechis, S. K.; Verdine, G. L. Nucleotide-dependent domain movement in the ATPase domain of a human type IIA DNA topoisomerase. *J. Biol. Chem.* **2005**, *280*, 37041–37047.
- (7) Wu, C.; Li, T.; Farh, L.; Lin, L.; Lin, T.; Yu, Y.; Yen, T.; Chiang, C.; Chan, N. Structural Basis of Type II Topoisomerase Inhibition by the Anticancer Drug Etoposide. *Science* **2011**, *333*, 459–462.
- (8) Moreland, J.; Gramada, A.; Buzko, O.; Zhang, Q.; Bourne, P. The Molecular Biology Toolkit (MBT): A modular platform for developing molecular visualization applications. *BMC Bioinf.* **2005**, *6*, No. 21.
- (9) De Luchi, D.; Tereshko, V.; Gouyette, C.; Subirana, J. A. Structure of the DNA coiled coil formed by d(CGATATATATAT). *ChemBioChem* **2006**, *7*, 585–587.
- (10) Pouliot, J. J.; Yao, K. C.; Robertson, C. A.; Nash, H. A. Yeast gene for a Tyr-DNA phosphodiesterase that repairs topoisomerase I complexes. *Science* **1999**, *286*, 552–555.
- (11) Wilson, D. M., III; Barsky, D. The major human abasic endonuclease: Formation, consequences and repair of abasic lesions in DNA. *Mutat. Res.* **2001**, *485*, 283–307.
- (12) Sirivolu, V. R.; Kumar, S.; Vernekar, V.; Marchand, C.; Naumova, A.; Cherugi, A.; Renaud, A.; Stephen, A. G.; Chen, F.; Sham, Y. Y.; Pommier, Y.; Wang, Z. 5-Arylideneethiothiazolidinones as Inhibitors of Tyrosyl–DNA Phosphodiesterase I. *J. Med. Chem.* **2012**, *55*, 8671–8684.
- (13) Coenye, T.; Vandamme, P., Eds. *Burkholderia: Molecular Microbiology and Genomics*; Horizon Bioscience: Norfolk, U.K., 2007; pp 153–177.
- (14) Daves, G. D.; Robins, R. K.; Cheng, C. C. Antibiotics. I. Synthesis of 1,6-Dimethyl-5,7-dioxo-1,5,6,7-tetrahydropyrimido [5,4-e] as-triazine (toxoflavin) and related Compounds. *J. Am. Chem. Soc.* **1962**, *84*, 1724–1729.
- (15) Wei, W.; Chua, M.-S.; Grepper, S.; So, S. Small molecule antagonists of Tcf4/ β -catenin complex inhibit the growth of HCC cells *in vitro* and *in vivo*. *Int. J. Cancer* **2010**, *126*, 2426–2436.
- (16) Showalter, H. D.; Turbiak, A. J.; Fearon, E. R.; Bommer, G. T. Pyrimidotriazinones and pyrimidopyrimidinones and methods of using the same. International Patent WO 2011166144, 2010.
- (17) Petry, S.; Barimghaus, K.-H.; Tennagels, N.; Guenter, M. Pyrimido[5,4-e][1,2,4]triazine-5,7-diones, methods for producing the same and their use. International Patent WO 20047737144, 2004.
- (18) Lacrampe, J. F.; Connors, R. W.; Ho, C. Y.; Richardson, A.; Freyne, E. J.; Buijsters, P. J.; Bakker, A. N. 3-furanyl analogs of toxoflavine as kinase inhibitors. International Patent WO 20047241763, 2004.
- (19) Essayan, D. M. Cyclic nucleotide phosphodiesterases. *J. Allergy Clin. Immunol.* **2001**, *108*, 671–680.
- (20) Meanwell, N. A. Synopsis of some recent tactical application of bioisosteres in drug design. *J. Med. Chem.* **2011**, *54*, 2529–2591.
- (21) Jaenchen, R.; Schonheit, P.; Thauer, R. K. Studies on the biosynthesis of coenzyme F420 in methanogenic bacteria. *Arch. Microbiol.* **1984**, *137*, 362–365.
- (22) Yoneda, F.; Sasaki, T. Preparation of 5-deazaflavin compounds as anticancer agents. Jpn. Kokai Tokkyo Koho, JP 199103081276 A 19910405, 1991.
- (23) Weissman, A. M.; Vousden, K. H.; Jensen, J. P.; Yang, Y.; Fang, S.; Woods, D.; Kenten, J. H.; Davydov, L.; Safiran, Y. J.; Oberoi, P. Deazaflavin compounds and methods of use thereof. International Patent WO 2004073615 A2 20040902, 2004.
- (24) Todorovic, N.; Giacomelli, A.; Hassell, J. A.; Frampton, C. S.; Capretta, A. Microwave-assisted synthesis of 3-aryl-pyrimido[5,4-e][1,2,4]triazine-5,7(1H,6H)-dione libraries: derivatives of toxoflavin. *Tetrahedron Lett.* **2010**, *51*, 6037–6040.
- (25) Chen, Y.; Barber, J. R.; Ng, S. C.; Zhou, Y. Parallel synthesis of novel 3-substituted 1-ethyl-6-methylpyrimido[4,5-c]pyridazine-5,7-(1H,6H)-dione analogs. *Synth. Commun.* **2010**, *40*, 821–832.
- (26) Prins, L. H. A.; Petzer, J. P.; Malan, S. F. Synthesis and *in vitro* evaluation of pteridine analogues as monoamine oxidase B and nitric oxide synthase inhibitors. *Bioorg. Med. Chem.* **2009**, *17*, 7523–7530.
- (27) Styles, V. L.; Morrison, R. W. Pyrimido[4,5-]pyridazines. Cyclizations with α -Keto Acids. *J. Org. Chem.* **1982**, *47*, 585–587.
- (28) Danter, W.; Threlfall, C.; Guizzetti, S.; Marin, J. Compounds and method for treatment of HIV. International Patent WO 2011120153, 2011.
- (29) Whitteck, J. T.; Ni, W.; Griffin, B. M.; Eliot, A. C.; Thomas, P. M.; Kelleher, N. L.; Metcalf, W. W.; van der Donk, W. A. Reassignment of the structure of the antibiotic A53868 reveals an unusual amino dehydrophosphonic acid. *Angew. Chem., Int. Ed.* **2007**, *46*, 9089–9092.
- (30) Bey, E.; Marchais-Oberwinkler, S.; Werth, R.; Negri, M.; Al-Soud, Y. A.; Kruchten, P.; Oster, A.; Frotscher, M.; Birk, B.; Hartmann, R. W. Design, synthesis, biological evaluation and pharmacokinetics of bis(hydroxyphenyl) substituted azoles, thiophenes, benzenes, and azabenzene as potent and selective nonsteroidal inhibitors of 17 β -hydroxysteroid dehydrogenase type 1 (17 β -HSD1). *J. Med. Chem.* **2008**, *51*, 6725–6739.
- (31) King, J. A.; Keown, J.; McIlroy, J. W.; Armstrong, W. P.; McKerver, M. A.; McMordie, A. Di-steroidal prodrugs of estradiol. U.S. Patent US 20050159399 A1 20050721, 2005.
- (32) Arhin, F.; Bélanger, O.; Ciblat, S.; Dehbi, M.; Delorme, D.; Dietrich, E.; Dixit, D.; Lafontaine, Y.; Lehoux, D.; Liu, J.; McKay, G.

A.; Moeck, G.; Reddy, R.; Rose, Y.; Srikumar, R.; Tanaka, K. S. E.; Williams, D. M.; Gros, P.; Pelletier, J.; Parr, T. R., Jr.; Far, A. R. A new class of small molecule RNA polymerase inhibitors with activity against Rifampicin-resistant *Staphylococcus aureus*. *Bioorg. Med. Chem.* **2006**, *14*, 5812–5832.

(33) Quiroga, J.; Trilleras, J.; Insuasty, B.; Abonía, R.; Noguera, M.; Marchal, A.; Cobo, J. A straightforward synthesis of pyrimido[4,5-b]quinoline derivatives assisted by microwave irradiation. *Tetrahedron Lett.* **2010**, *51* (7), 1107–1109.

(34) Wilson, J. M.; Henderson, G.; Black, F.; Sutherland, A.; Ludwig, R. L.; Vousden, K. H.; Robins, D. J. Synthesis of 5-deazaflavin derivatives and their activation of p53 in cells. *Bioorg. Med. Chem.* **2007**, *15* (1), 77–86.

(35) Yoneda, F.; Nagamatsu, T. A convenient synthesis of toxoflavins, toxflavin 4-oxides and 1-demethyltoxoflavins. *Chem. Pharm. Bull.* **1975**, *23*, 2001–2009.

(36) Wempen, I.; Fox, J. J. Pyrimidines. II. Synthesis of 6-fluorouracil. *J. Med. Chem.* **1964**, *7* (4), 207–209.

(37) Baker, B. R.; Rzeszutowski, W. Irreversible enzyme inhibitors. CXXI. Thymidine phosphorylase. 9. Nature and dimensions of the hydrophobic bonding region. *J. Med. Chem.* **1968**, *11*, 639–644.

(38) Wright, G. E.; Brown, N. C. Inhibitors of *Bacillus subtilis* DNA polymerase III. 6-Anilinouracils and 6-(alkylamino)uracils. *J. Med. Chem.* **1980**, *23*, 34–38.

(39) Wright, G. E.; Gambino, J. J. Quantitative structure-activity relationships of 6-anilinouracils as inhibitors of *Bacillus subtilis* DNA polymerase III. *J. Med. Chem.* **1984**, *27*, 181–185.

(40) McCaffrey, R.; Wright, G.; Baril, E. F. Composition and method for inhibiting terminal deoxyribonucleotidyl transferase activity in cancer chemotherapy. U.S. Patent 4,576,948 A, 1986.

(41) Shinkai, S.; Kawase, A.; Yamaguchi, T.; Manabe, O.; Wada, Y.; Yoneda, F.; Ohta, Y.; Nishimoto, K. Coenzyme models. 47. Synthesis and reactivity studies of novel flavinophanes and 5-deazaflavinophanes: correlation between flavin reactivity and ring strain. *J. Am. Chem. Soc.* **1989**, *111*, 4928–4935.

(42) Shinkai, S.; Yamaguchi, T.; Nakao, H.; Manabe, O. Synthesis of new deazaflavins with planar chirality. Redox-induced “rope-skipping” racemization. *Tetrahedron Lett.* **1986**, *27*, 1611–1614.

(43) Brown, N. C.; Barnes, M. H.; Wright, G. E. Compounds destabilizing the zinc finger of the dnaE protein of Gram-positive bacteria and their use as antibiotics. International Patent WO 2000020556 A2, 2000.

(44) Thomson, G. J.; Hamilton, N. S.; Hopkins, G. V.; Waddell, I. D.; Watson, A. J.; Ogilvie, D. J. A fluorescence based assay for the AP-site cleavage activity of human tyrosyl DNA phosphodiesterase 1. *Anal. Biochem.* **2013**, *440*, 1–5.

(45) Calculated log *P* determined using Dotmatics software (www.dotmatics.com).

(46) Permeability assessed in Caco-2 membrane assay: $P_{a \rightarrow b}$ 0.9×10^{-6} cm s⁻¹; efflux ratio 49.1.

(47) Schrödinger Suite 2012, Schrödinger, LLC, New York, NY, 2012.

(48) TorchV10, part of the Cresset software package, <http://www.cresset-group.com/products/torch/>

(49) SparkV10, part of the Cresset software package, www.cresset-group.com/products/spark/. The Spark uses a fragment database to suggest replacements for a user defined scaffold in order to identify moieties that reproduce the shape and electrostatic and hydrophobic properties of the parent compound.

(50) Thorne, N.; Auld, D. S.; Inglese, J. Apparent activity in high-throughput screening: Origins of compound-dependent assay interference. *Curr. Opin. Chem. Biol.* **2010**, *14*, 315–324.

(51) Soares, K. M.; Blackmon, N.; Shun, T. Y.; Shinde, S. N.; Takyi, H. K.; Wipf, P.; Lazo, J. S.; Johnston, P. A. Profiling the NIH Small Molecule Repository for compounds that generate H₂O₂ by redox cycling in reducing environments. *Assay Drug Dev. Technol.* **2010**, *8*, 152–174.

(52) Schellenberg, M. J.; Appel, C. D.; Adhikari, S.; Robertson, P. D.; Ramsden, D. A.; Williams, R. S. Mechanism of repair of 5'-

topoisomerase II-DNA adducts by mammalian tyrosyl-DNA phosphodiesterase 2. *Nat. Struct. Mol. Biol.* **2012**, *19*, 1363–1371.

(53) Shi, K.; Kurahashi, R. G.; Tsutakawa, S. E.; Tainer, J. A.; Pommier, Y.; Aihara, H. Structural basis for recognition of 5'-phosphotyrosine adducts by Tdp2. *Nat. Struct. Mol. Biol.* **2012**, *19*, 1372–1377.

(54) Nagamatsu, T.; Yamasaki, H. General syntheses of 1-alkyltoxoflavin and 8-alkylfervenulin derivatives of biological significance by the regioselective alkylation of reumycin derivatives and the rates of transalkylation from 1-alkyltoxoflavins into nucleophiles. *J. Chem. Soc., Perkin Trans.* **2001**, *1*, 130–137.

(55) Blehaut, H.; Bellamy, F.; Matt, C.; Giraud, S.; Charre, D.; Inhibitors of cystathionine beta synthase to reduce the neurotoxic overproduction of endogenous hydrogen sulfide. International Patent WO2010072807 (A2), 2010.